

Mineral compositions and magmatic evolution of the calcalkaline rocks of northwestern Sardinia, Italy

Vincenza Guarino^{1,*}, Lorenzo Fedele¹, Luigi Franciosi¹, Roberto Lonis², Michele Lustrino^{3,4},
Marianna Marrazzo¹, Leone Melluso¹, Vincenzo Morra¹, Ivana Rocco¹ and Fiorenzo Ronga¹

¹ Dipartimento di Scienze della Terra, Università degli Studi di Napoli Federico II,
Via Mezzocannone 8, 80134 Napoli, Italy

² Progemisa S.p.A., Via Contivecchi 7, 09122 Cagliari, Italy

³ Dipartimento di Scienze della Terra, Università degli Studi di Roma La Sapienza,
P.le A. Moro 5, 00185 Roma, Italy

⁴ CNR - Istituto di Geologia Ambientale e Geoingegneria (IGAG), Roma, Italy

*Corresponding author: vincenza.guarino@unina.it

Abstract

During Early Miocene northwestern Sardinia was interested by widespread volcanic activity belonging to the calcalkaline to high-K calcalkaline “orogenic” Sardinian cycle. The peak of activity is recorded in the ~ 22–18 Ma time span and it is mostly concentrated along the *Fossa Sarda* graben, an Oligo-Miocene rift system cutting the western Sardinia from north to south. The northwestern Sardinia volcanic rocks crop out in the districts of Bosa-Alghero, Anglona, Logudoro, Mulargia-Macomer and Ottana graben, ranging in composition from rare high alumina basalts to rhyolitic ignimbrites (welded and unwelded) and lava flows, through basaltic andesites, andesites and dacitic domes, with the most evolved rocks (dacites and rhyolites) being volumetrically predominant.

Here we report the chemical composition of the main rock-forming minerals (clinopyroxene, orthopyroxene, plagioclase, sanidine, magnetite, ilmenite, olivine, brown mica and amphibole) and whole-rock data covering the entire spectrum of occurring lithotypes.

The bulk-rock major and trace element variations are consistent with an evolution mainly driven by fractional crystallization of the observed mineral phases. This was confirmed by mass balance calculations and MELTS-based modelling, which allowed reconstructing liquid lines of descent for each district. Crystallization conditions took place at low pressures (1 kbar) and low H₂O contents (< 2 wt.%), with oxygen fugacities close to the QFM and Ni-NiO synthetic buffers and temperature values ranging from ~ 900 to ~ 1150 °C for mafic rocks and from ~ 800 to ~ 1000 °C for the silicic ones. Open-system processes may also have had a role in the petrogenesis of the silicic rocks.

Key words: ignimbrites; mineral chemistry; orogenic magmatism; Sardinia.

Introduction

During the Cenozoic an intense igneous activity with calcalkaline to high-K calcalkaline products took place in Sardinia (Coulon et al., 1974; Montigny et al., 1981; Beccaluva et al., 1985; Morra et al., 1994; 1997; Brotzu et al., 1997a; 1997b; Lustrino et al., 2004; 2009; 2011; Conte et al., 2010, and references therein). The volcanic products comprise pyroclastic flow deposits, lava flows and domes; their compositions are dominated by dacites and rhyolites, with subordinate andesites and very scarce basalts.

Despite the interest raised by the Sardinian igneous rocks in the last ~15-20 years, some key aspects remain to be investigated in detail. Indeed, most recent literature is focused on primitive magmatic compositions and their relationships with a subduction-modified mantle source (Brotzu et al., 1997a; 1997b; Morra et al., 1997; Mattioli et al., 2000; Downes et al., 2001; Franciosi et al., 2003; Conte et al., 2010), whereas the petrogenesis of the more widespread silicic products is basically that produced during '60s and '70s (e.g., Deriu, 1962; Coulon et al., 1973; 1978; Lonis et al., 1997). This study is intended to fill this gap by presenting a new set of data set for the calcalkaline volcanic rocks cropping out in the northwestern sector of Sardinia, where silicic lithologies are particularly abundant. This investigation is focused on the mineralogical characterization and on the evaluation of the physico-chemical environment of crystallization.

Geodynamic and geological background

Up to Early Oligocene times the Sardinia-Corsica micro-plate was contiguous with the southern European margin (Provence, France, and Catalonia, Spain; e.g., Cherchi et al., 2008; Dieni et al., 2008; Lustrino et al., 2009; Carminati et al., 2010, and references therein).

During the Late Oligocene, with the opening of Ligurian-Provencal Basin, the Sardinia-Corsica micro-plate rifted toward SE and then drifted counter-clockwise away from the southern Europe paleo-margin, with a rotation pole located around the present gulf of Genoa (NW Italy; Carminati et al., 1998; 2010; Jolivet et al., 1998; Speranza et al., 2002; Gattacceca et al., 2007; Lustrino et al., 2009). The continental rifting phase started ~ 30 Ma, whereas the drifting phase started around ~ 22 Ma until ~ 15 Ma, after a counter clock-wise rotation of ~ 60 degrees (Gueguen et al., 1998; Speranza et al., 2002; Vigliotti and Langenheim, 1995; Schettino and Turco, 2006; Lustrino et al., 2009; Carminati et al., 2010). From Langhian (~ 15 Ma) the Sardinia-Corsica micro-plate reached its present position and the extensional tectonics shifted eastwards, leading to the development of Tyrrhenian Sea and the Apennine fold-and-thrust belt (Lustrino et al., 2009; Carminati et al., 2010, and references therein).

In this complex geodynamic scenario, the island of Sardinia experienced an intense magmatism (Lecca et al., 1997; Lustrino et al., 2004; 2009; 2011) which can be chronologically and geochemically divided into two distinct phases. The products of the oldest phase (Late Eocene-Middle Miocene activity, or LEMM; ~ 38-13 Ma; Lustrino et al., 2009, and references therein) show "orogenic" (i.e., subduction-related) geochemical signature, whereas the products of the youngest phase (Late Miocene-Quaternary, hereafter LMQ; ~ 12-0.1 Ma) show "anorogenic" (within plate) geochemical characteristics (e.g., Beccaluva et al., 1985; Lustrino et al., 2004; 2007a; 2007b; 2009; 2011; Lustrino and Wilson, 2007, and references therein).

The volume of the erupted magma amounts to ~ 1000-2500 km³, excluding the volume of rocks deposited along the submerged margins of the island, hypothesizing an originally continuous pyroclastic flow cover in northern Sardinia (with an areal extent of ~ 4800 km² and an average

thickness in the range of 200-500 m). Such a large amount of magma was produced, in a relatively short time span, and may have had significant effects on marine ecosystem of the area (e.g., Brandano et al., 2010; Brandano and Policicchio, 2011). As for the products emplaced in the northwestern sector, Deriu (1962) first proposed a stratigraphic and mineral-petrographic subdivision taking into account four stratigraphic sequences: 1) the *andesitoide inferiore* (lower andesitic) series; 2) the *trachitoide inferiore* (lower trachytic) series, the first evidence of acid volcanism with ignimbritic facies; 3) the *andesitoide superiore* (upper andesitic) series, characterized by the intercalation of fluvial-lacustrine sediments and pyroclastic materials; 4) the *trachitoide superiore* (upper trachytic) series, characterized by erosive features and intercalations of fluvial-lacustrine sediments. Coulon (1977) provided a detailed volcano-stratigraphic, mineralogical and petrologic description (from base to top): 1) the *andesitica inferiore* (lower andesitic) series, characterized by products with basalt and basaltic andesite composition with minor dacites and rhyolites; 2) the *ignimbritica inferiore* (lower ignimbritic) series; 3) the *andesitica superiore* (upper andesitic) series; 4) the *dactic domes* and *rhyolitic lava flows*; 5) the *ignimbritica superiore* (upper ignimbritic) series and 6) the *andesitica terminale* (upper andesitic) series, with basaltic andesites, dacites and rhyolites. More recent studies (i.e., Lecca et al., 1997) still rely on this stratigraphic schemes.

The LEMM products range in composition from dacites to rhyolites, with subordinate basaltic andesites, andesites, high-Al basalts and rare high-Mg basalts and belong to the calc-alkaline and high-K calc-alkaline series (e.g., Brotzu et al., 1997a; 1997b; Lecca et al., 1997; Lonis et al., 1997; Morra et al., 1997; Downes et al., 2001; Lustrino et al., 2004; 2009; Conte et al., 2010). Rare peralkaline products (comendites) are found in southwestern Sardinia (Sulcis; Araña

et al., 1974; Morra et al., 1994).

The mantle source of the mafic “orogenic” volcanic rocks is in the wedge above a west-directed oceanic lithosphere subducted below the southern European continental margin, enriched in large ion lithophile elements by fluids/melts derived from the subducted slab (Franciosi et al., 2003; Lustrino et al., 2004; 2009; 2011).

Analytical techniques

The samples were cut with a saw and crushed in a jaw crusher. The obtained chips were washed in distilled water and then ground in a low-blank agate mortar and analyzed for major and trace elements were obtained with XRF (X-Ray fluorescence) on pressed powder pellets at CISAG (Centro Interdipartimentale di Servizi per Analisi Geomineralogiche), University of Napoli Federico II (see Melluso et al., 2005 for details). Mineral compositions were obtained at IGAG-CNR, Rome, using a Cameca SX50 electron microprobe equipped with five spectrometers and at CISAG, with an Oxford Instruments Microanalysis Unit, equipped with an INCA X.act detector and a JEOL JSM-5310 microscope operating at 15 kV primary beam voltage, 50-100 μ A filament current, variable spot size and 50 s net acquisition time (see Melluso et al., 2010 and Guarino et al., 2011 for full details).

Classification and geochemical features

The Early Miocene volcanic rocks subject of this study were collected in five districts in the northwestern sector of Sardinia (Figure 1a, b). The district, the number of samples, the lithologies and the absolute ages for each of them are summarized in Table 1.

Table 2 shows major and trace element composition of representative Early Miocene rocks from northwestern Sardinia. According to the TAS diagram (Figure 2a), the rocks are

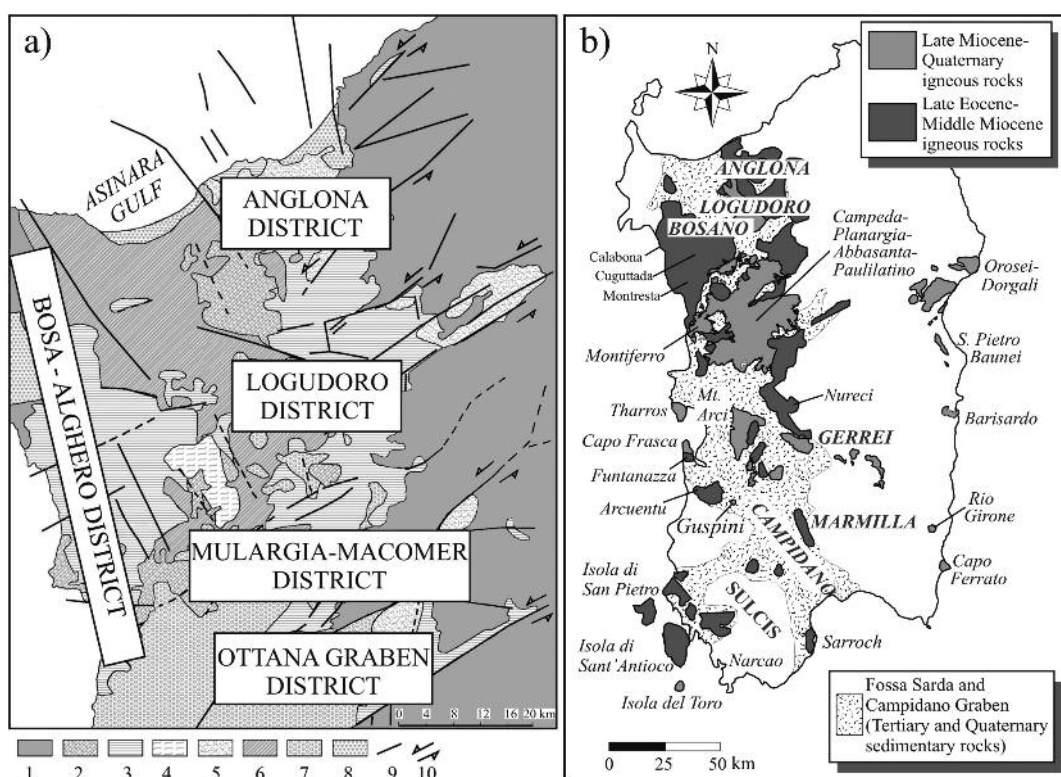


Figure 1. a) Geological sketch map (modified after Sau et al., 2005) for the studied districts of the Late Eocene-Middle Miocene Sardinia magmatic phase. 1 = Palaeozoic basement; 2 = Early Miocene andesites; 3 = Early Miocene ignimbrites; 4 = rhyodacitic lavas; 5 = fluvial-lacustrine and epiclastic complex of Miocene basins; 6 = marine sequences of Miocene basins; 7 = anorogenic volcanites of the Late Miocene-Quaternary cycle; 8 = Quaternary sedimentary deposits; 9 = fault zones; 10 = main transcurrent movements. b) Simplified geological sketch map of Sardinia (modified after Lustrino et al., 2009).

mainly dacites and rhyolites, with subordinate basalts, basaltic andesites and andesites. A bimodal composition is indicated by a Daly gap, with andesitic compositions ($\text{SiO}_2 = 57\text{-}63 \text{ wt.\%}$) being rare.

Among the mafic lithotypes, the few basalts, from the Bosa-Alghero and Logudoro districts, show high Al_2O_3 (17.8-19.4 wt.%) and relatively low MgO (3.4-7.2 wt.%), Mg\# [0.41-0.60; $\text{Mg\#} = \text{molar MgO}/(\text{MgO}+\text{FeO}+\text{MnO})$], Cr (16-52.4 ppm) and Ni (9.0-19 ppm). These basalts are

classified as high-Al basalts (HAB) according to Kersting and Arculus (1994). The basaltic rocks at Montresta (Figure 1b), are classified as high-Mg basalts (HMB; Morra et al., 1997; Franciosi et al., 2003), due to high MgO (up to 11 wt.%) and relatively low Al_2O_3 (< 16 wt.%).

Metaluminous [$\text{Al}_2\text{O}_3/(\text{CaO}+\text{Na}_2\text{O}+\text{K}_2\text{O}) < 1$] and peraluminous [$\text{Al}_2\text{O}_3/(\text{CaO}+\text{Na}_2\text{O}+\text{K}_2\text{O}) > 1$] dacites and rhyolites are present (Figure 2b); no peralkaline rhyolites or trachytes have been found in northern Sardinia.

Table 1. Synoptic table showing district, number of samples, main lithologies and absolute ages of the studied Early Miocene rocks from northwestern Sardinia.

District	Number of samples	Lithology	Age
Bosa-Alghero district	10	basalts, basaltic andesite lava flows	~ 28-16 Ma (Montigny et al., 1981; Beccaluva et al., 1985; Lecca et al., 1997; Deino et al., 2001; Gattacceca et al., 2007)
	1	andesitic lava flows	
	39	welded and unwelded ignimbrites	
Anglona district	2	andesitic lava flows	~ 21-18 Ma (Montigny et al., 1981; Lecca et al., 1997; Oudet et al., 2010)
	5	welded and unwelded ignimbrites	
Logudoro district	6	basalts and basaltic andesite lava flows	
	1	andesitic lava flows	~ 25-17 Ma
	5	dacitic domes	(Coulon et al., 1974; Beccaluva et al., 1985)
	1	rhyolitic lava flows	
Mulargia-Macomer district	26	welded and unwelded ignimbrites	
	1	rhyolitic lava flows	~ 21.8-21.6 Ma; (Lecca et al., 1997 and references therein)
	5	welded and unwelded ignimbrites	
Ottana graben district	3	welded and unwelded ignimbrites	~ 21-19.4 Ma (Lecca et al., 1997 and references therein)

The analyzed rocks display smooth and linear variation trends (Figure 3) characterized by decreasing TiO_2 , Al_2O_3 , Fe_2O_3 , MgO and CaO with increasing SiO_2 . The trace elements Rb, Ba, Y and Zr, increase with silica, then their concentrations suddenly decrease at ~70% SiO_2 . Sr decreases with increasing SiO_2 (Figure 4).

Petrographic features

The main petrographic features of Early Miocene rocks of northwestern Sardinia are reported in Figure 5 and are briefly summarized below.

Basalts. The rocks (from the Bosa-Alghero and Logudoro districts) are porphyritic. The main phenocrysts are subhedral to euhedral zoned plagioclase (sometimes with rounded rims), and clinopyroxene, generally showing rounded rims, only sporadically subhedral in shape. Olivine is quite common and shows euhedral shapes often corroded or iddingsitized. Opaque oxides mainly occur as inclusions or in the groundmass. The groundmass is microcrystalline and it is made of the same phases observed as phenocrysts (except olivine) plus rare orthopyroxene.

Basaltic Andesites. The rocks (Bosa-Alghero,

Table 2. Major (wt.%) and trace element (ppm) concentrations, and CIPW normative minerals for representative samples of Early Miocene rocks from northwestern Sardinia.

Locality	Mte Riuju-M. M.te Majore	Montresta	Mt. Fare	Pta Tripides	Mt. Fare	Pta	Mt. Fare	Mt. Minerva	Mt. Minerva	Mt. Minerva	Bosa	Mt. Minerva
	N 40°25'22" N 40°23'12" N 40°21'39" N 40°21'45"	N 40°21'58" N 40°26'12" N 40°21'48" N 40°30'22" N 40°26'36" N 40°33'38" N 40°22'54"	N 40°21'58" N 40°26'12" N 40°21'48" N 40°30'22" N 40°26'36" N 40°33'38" N 40°22'54"	N 40°21'58" N 40°26'12" N 40°21'48" N 40°30'22" N 40°26'36" N 40°33'38" N 40°22'54"	SW Mt. Mannu							
G.P.S. coordinates	E 08°25'02" E 08°30'19" E 08°25'54" E 08°25'56"	HAB	HAB	HAB	BA							
Rock type	HAB	HAB	HAB	MARA23	MARA25	MARA23	MARA34	MARA33	MARA36	MARA13	MARA22	MARA12
XRF (wt.%)	MA23	MA21	MA23	MA23	MA23	MA23	MA23	MA23	MA23	MA23	MA29B	MA35
SiO ₂	47.98	48.12	51.27	51.93	53.34	53.90	60.87	65.28	69.37	70.34	71.51	73.61
TiO ₂	1.24	1.11	0.99	0.91	0.96	0.70	0.46	0.66	0.64	0.41	0.30	0.28
Al ₂ O ₃	18.85	17.78	18.26	18.74	19.27	16.37	15.85	14.35	13.59	14.50	13.22	13.18
Fe ₂ O ₃	10.69	11.27	10.23	10.23	9.29	10.09	6.73	4.93	5.41	3.88	2.92	2.70
MnO	0.18	0.20	0.20	0.21	0.19	0.13	0.06	0.12	0.06	0.10	0.05	0.03
MgO	7.15	5.90	4.34	4.02	2.87	5.48	3.75	0.77	0.76	0.75	1.38	0.31
CaO	10.42	11.87	10.56	9.83	9.65	8.67	6.74	4.75	2.29	2.80	2.58	1.98
Na ₂ O	2.11	2.32	2.63	2.88	3.12	2.61	2.13	2.76	3.97	3.31	3.09	2.63
K ₂ O	1.14	1.22	1.26	1.01	1.12	1.51	2.11	3.49	3.66	4.36	3.89	3.78
P ₂ O ₅	0.23	0.20	0.26	0.16	0.23	0.22	0.15	0.18	0.17	0.14	0.12	0.08
Mg# [#]	0.60	0.53	0.48	0.46	0.43	1.48	4.40	2.46	1.81	3.60	1.33	5.77
LOI	1.64	0.59	0.57	0.86								
XRF (ppm)					100	100	100	100	100	100	100	100
Sc	40	32	34	35	29	32	23	19	13	13	11	7
V	375	313	266	290	251	231	159	62	74	34	36	47
Cr	52	45	29	16	21	29	4	11	1	1		
Ni	9	19	9	11	11	11	9	5	3	3	5	1
Rb	33	35	30	31	29	39	45	127	135	161	152	125
Sr	492	366	329	318	327	300	291	286	202	187	194	144
Y	29	26	24	26	24	29	30	32	55	32	31	45
Zr	89	73	71	84	74	103	158	237	251	202	229	273
Nb	1.6	4.9	4.5	4.9	4.1	7.2	13.6	9.7	15.2	12.3	12.6	14.4
Ba	137	134	177	206	202	219	819	607	649	533	680	892
CIPW norms:												
<i>quartz</i>												
<i>corundum</i>												
<i>orthoclase</i>	6.75	7.22	7.45	5.97	6.63	8.93	12.49	20.59	21.60	21.07	25.74	1.16
<i>albite</i>	17.88	19.65	22.27	24.39	26.43	22.11	18.05	23.39	33.55	28.05	26.18	22.97
<i>anorthite</i>	38.57	34.48	34.27	35.20	35.25	28.47	27.42	16.46	8.48	12.99	9.31	9.51
<i>diopside</i>	9.53	19.09	13.65	10.44	9.35	10.81	4.13	4.82	1.53	2.32		
<i>hypersthene</i>	9.82	0.02	16.65	17.44	13.91	20.77	17.60	13.01	7.61	5.43	7.01	4.04
<i>olivine</i>	11.78	14.03										
<i>magnetite</i>	1.84	1.94	1.76	1.60	1.74	1.16	0.85	0.93	0.67	0.66	0.50	0.47
<i>ilmenite</i>	2.36	2.11	1.88	1.73	1.83	1.33	0.78	1.26	1.02	0.78	0.57	0.53
<i>apatite</i>	0.55	0.47	0.62	0.38	0.55	0.52	0.36	0.43	0.40	0.33	0.28	0.12
<i>sum</i>	99.1	99.0	99.1	99.2	99.1	99.2	99.4	99.6	99.5	99.7	99.7	99.8

The major oxide analyses are recalculated to 100 wt.% LOI-free. HAB = high alumina basalt; BA = basaltic andesite; A = andesite; D = dacite; R = rhyolite. Weight loss on ignition (LOI, in wt.%) was determined by standard thermo-gravimetric method.

Table 2. Continued...

Logudoro district

Locality	Thiesi	Ituri	Thiesi	S. Mt. Frusciu	Logudoro district						Mte Traessu-	Cossone	Thiesi			
					HAB	HAB	HAB	MA19	MA19	MA12	MA11	MA11	MA13A	MA13B		
G.P.S. coordinates E 08° 39' 16"E 08° 37' 38"	N 40° 33' 01"N 40° 23' 49"	N 40° 28' 09"N 40° 28'51"	N 40° 29'53"	N 40° 30'28"	N 40° 30'28"	N 40° 31'57"	N 40° 28'34"	N 40° 28'35"	N 40° 28'34"							
Rock type XRF (wt%)	HAB	HAB	HAB	MA19	MA19	MA72A	MA12	MA11	MA11	MA13A	MA13B	MA50	MA37	MA36	R	
SiO ₂	49.93	51.54	51.81	54.70	55.70	61.23	69.73	70.06	72.42	73.28	75.93	76.66	77.42		R	
TiO ₂	0.93	1.01	0.83	1.04	0.81	0.77	0.46	0.42	0.36	0.26	0.18	0.17	0.17		R	
Al ₂ O ₃	19.43	17.82	18.78	19.09	16.51	16.55	14.05	14.10	13.20	13.30	12.09	11.75	11.82		R	
Fe ₂ O ₃	10.72	10.76	10.32	9.74	8.46	7.25	3.56	3.42	2.71	2.70	2.16	2.05	2.04		R	
MnO	0.13	0.19	0.20	0.06	0.15	0.09	0.07	0.08	0.04	0.02	0.07	0.05	0.04		R	
Mg#	3.39	4.49	4.66	0.86	4.48	1.10	1.48	1.44	0.86	0.25	0.53	0.22	1.16		R	
LOI	1.89	1.86	1.84	1.34	1.27	1.74	2.56	2.45	0.72	0.80	3.45	0.56	6.20		R	
XRF (ppm)																
Sc	30	27	32	29	25	25	11	7	9	9	2	4	4		R	
V	317	266	239	415	195	190	37	38	25	25					R	
Cr	33	24	15	23	30	24	4	5	5	5	1		3		R	
Ni	18	16	13	6	13	12	0	3	2	2					R	
Rb	48	39	34	84	85	126	141	151	144	144	178	180	140		R	
Sr	462	540	357	389	450	434	269	256	237	237	144	114	206		R	
Y	24	24	21	18	24	31	30	30	29	29	29	27	13		R	
Zr	72	91	66	82	150	205	234	227	210	210	186	180	111		R	
Nb	1.1	0.6	1.8	2.4	4.4	6.2	12.1	11.6	11.1	11.1	14.8	14.6	8.2		R	
Ba	155	243	184	235	288	388	633	601	647	647	484	509	569		R	
CIPW norms:																
quartz																
corundum																
orthoclase	7.81	8.88	6.03	13.08	15.74	20.48	24.27	23.14	24.91	41.30	27.87	28.93	1.73		R	
albite	23.46	25.59	22.44	19.49	23.21	25.68	24.83	26.18	25.59	18.13	24.74	26.94	22.66		R	
anorthite	36.67	30.62	36.31	35.23	24.87	21.32	13.04	13.02	9.99	4.41	5.95	3.29	13.64		R	
diopside	14.52	11.92	8.49	10.44	12.30	7.51	2.69	2.32	3.63	0.22	1.04	8.98			R	
hypersthene	6.90	15.23	20.40	8.34	15.50	7.63	6.55	6.54	3.49	3.90	3.98	2.61	5.46		R	
olivine	5.59	2.44													R	
magnetite	1.85	1.86	1.78	1.68	1.46	1.25	0.61	0.59	0.47	0.47	0.37	0.35	0.35		R	
ilmenite	1.77	1.92	1.58	1.98	1.54	1.46	0.88	0.80	0.68	0.49	0.34	0.32	0.32		R	
apatite	0.50	0.62	0.36	0.38	0.47	0.45	0.33	0.28	0.17	0.14	0.12	0.09	0.09		R	
sum	99.1	99.1	99.2	99.2	99.3	99.4	99.7	99.7	99.8	99.8	99.8	99.8	99.8	99.8		R

The major oxide analyses are recalculated to 100 wt% LOI-free. HAB = high alumina basalt; BA = basaltic andesite; A = andesite; D = dacite; R = rhyolite. Weight loss on ignition (LOI, in wt.%) was determined by standard thermo-gravimetric method.

Table 2. Continued...

Locality	Anglona district				Mulargia - Macomer district				Ottana graben district			
	Sedini	Castelsardo	Mt. S. Padre	Ab. Mulargia	Mt. S. Padre	N 40°17'20"	N 40°17'52"	N 40°17'20"	N 40°14'19"	N 40°13'34"		
G.P.S. coordinates	N 40°50'54" E 08°24'06"	N 40°51'42" E 08°27'42"	N 40°54'47" E 08°41'58"	N 40°17'06" E 08°49'28"	N 40°17'53" E 08°48'36"	N 40°17'52" E 08°50'30"	N 40°17'20" E 09°02'46"	N 40°17'20" E 09°03'27"	N 40°14'19" E 09°01'54"	N 40°13'34" E 09°01'54"		
Rock type XRF (wt.%)	A MA82	D MA84B	R MA6A	R MA65	R MA61	D MA62A	R MA69	R MA67	R MA66			
SiO ₂	56.58	66.86	75.96	69.21	71.73	72.93	68.84	72.60	76.75			
TiO ₂	0.83	0.57	0.40	0.56	0.48	0.37	0.72	0.47	0.34			
Al ₂ O ₃	16.51	14.80	11.63	14.90	13.48	13.10	13.71	12.85	10.90			
Fe ₂ O ₃	8.93	5.31	2.55	4.35	4.10	3.67	5.57	4.15	3.19			
MnO	0.15	0.11	0.04	0.12	0.07	0.06	0.04	0.04	0.03			
MgO	2.99	1.95	0.19	0.97	0.25	0.53	0.81	0.44	0.19			
CaO	8.65	2.91	1.33	1.92	1.14	1.29	2.81	1.84	1.18			
Na ₂ O	2.64	3.36	3.49	3.86	3.62	3.57	3.59	3.52	3.23			
K ₂ O	2.51	3.98	4.32	4.00	5.06	4.38	3.73	3.98	4.09			
P ₂ O ₅	0.20	0.15	0.08	0.12	0.07	0.09	0.18	0.11	0.08			
sum	100	100	100	100	100	100	100	100	100	100		
Mg# LOI	1.17	5.13	0.64	2.08	1.00	1.38	2.95	2.21	1.25			
XRF (ppm)												
Sc	31	15	10	16	12	15	22	17	10			
V	245	39	1	40	34	8	96	23	13			
Cr	16		2	5	2	2			1			
Ni	9	8	1	5	5		3		1			
Rb	104	306	147	130	148	155	116	140	146			
Sr	364	258	119	164	120	116	238	144	100			
Y	25	52	38	41	34	47	43	37	43			
Zr	119	283	243	221	244	279	229	260	254			
Nb	4.7	14.4	16.1	13.5	15.1	17.5	13.8	16.5	16.2			
Ba	372	604	502	496	515	571	1269	551	554			
CIPW norms:												
quartz	7.55	20.45	35.50	23.91	26.45	30.05	24.59	30.56	38.41			
corundum		0.04		1.03	0.13	0.35						
orthoclase	14.85	23.50	25.50	23.61	29.88	25.86	22.03	23.49	24.20			
albite	22.36	28.39	29.56	32.62	30.67	30.25	30.35	29.82	27.36			
anorthite	25.76	13.48	3.32	8.75	5.21	5.82	10.29	7.49	3.14			
diopsidic	13.28		2.41				2.10	0.80	1.92			
hypersthene	11.82	11.33	2.10	7.62	5.52	5.81	7.39	5.61	3.30			
olivine												
magnetite	1.54	0.92	0.44	0.75	0.71	0.63	0.96	0.71	0.55			
ilmenite	1.58	1.08	0.76	1.06	0.91	0.70	1.37	0.89	0.65			
apatite	0.47	0.36	0.19	0.28	0.17	0.21	0.43	0.26	0.19			
sum	99.2	99.5	99.8	99.6	99.6	99.7	99.5	99.6	99.7			

The major oxide analyses are recalculated to 100 wt.% LOI-free. HAB = high alumina basalt; BA = basaltic andesite; A = andesite; D = dacite; R = rhyolite. Weight loss on ignition (LOI, in wt.%) was determined by standard thermo-gravimetric method.

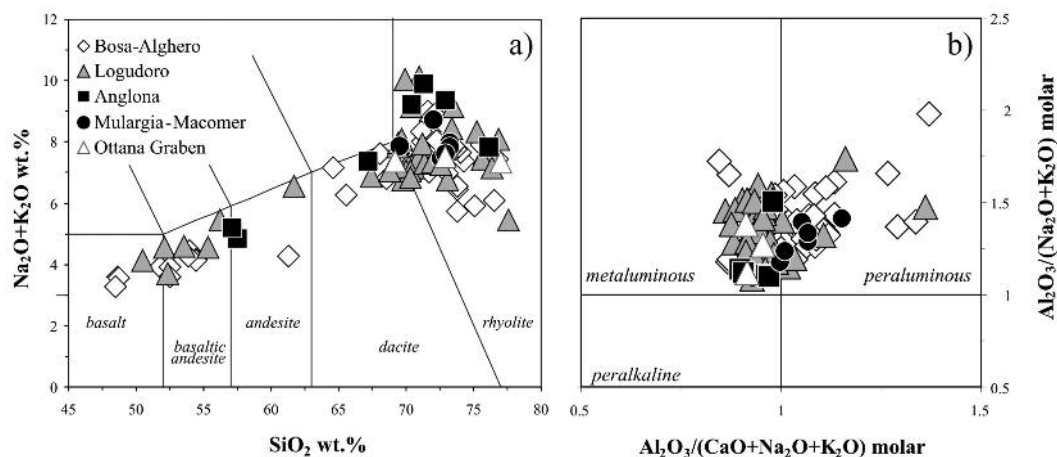


Figure 2. a) Total Alkali vs. Silica (TAS; Le Bas et al., 1986) classification diagram for the studied Early Miocene volcanic rocks from north western Sardinia. b) Molar $\text{Al}_2\text{O}_3/(\text{Na}_2\text{O}+\text{K}_2\text{O})$ vs. $\text{Al}_2\text{O}_3/(\text{CaO}+\text{Na}_2\text{O}+\text{K}_2\text{O})$ for the studied Early Miocene volcanic rocks from northwestern Sardinia.

Anglona and Logudoro districts) are porphyritic to glomeroporphyritic, with plagioclase being the predominant phenocryst. Clinopyroxene generally occurs as subhedral pheno- to microphenocrysts with rounded rims, sometimes completely altered. Olivine crystals are rare, often altered into haematite or iddingsite. Orthopyroxene is represented by rare euhedral and quite fractured crystals. Opaque oxides occur as inclusions within mafic minerals or in the groundmass. The groundmass is microcrystalline to intersertal, more rarely hypocrystalline, with microlites of plagioclase, clinopyroxene and opaque oxides.

Andesites. These rocks (Bosa-Alghero and Logudoro districts) are quite altered, with plagioclase and euhedral clinopyroxene phenocrysts. The groundmass is often argillified.

Dacitic domes. The dacites from Logudoro district are porphyritic for phenocrysts of plagioclase, clinopyroxene and occasionally opaque oxides. Clusters of plagioclase, clinopyroxene and oxides are sometimes noted. Brown mica (often altered), and euhedral green amphibole are common microlites. Orthopyroxene

is a rare microlite. Accessory apatite is found in the groundmass.

Rhyolitic lavas. The Logudoro rhyolites are porphyritic, with euhedral to subhedral plagioclase with altered cores. Abundant alkali feldspar, oxidized brown mica and minor amphibole plus opaque oxide microcrysts are also observed, set into a completely glassy groundmass with no evidences of devitrification. The Mulargia-Macomer rhyolites are porphyritic with subhedral zoned phenocrysts of plagioclase, microcrysts of opaque oxides, quartz and deeply altered mafic phases set into a microcrystalline groundmass mainly made of alkali feldspar, quartz and rare apatite crystals.

Ignimbrites outcrop in the Bosa-Alghero, Anglona, Logudoro, Mulargia-Macomer and Ottana graben districts. These ignimbrites (dacitic to rhyolitic in composition) can be subdivided into two types: a) *unwelded ignimbrites* and b) *welded ignimbrites*.

a) **Unwelded ignimbrites.** These samples are made up of glassy shards, pumices and scoria fragments. The observed mineral assemblages comprise rounded and variably zoned

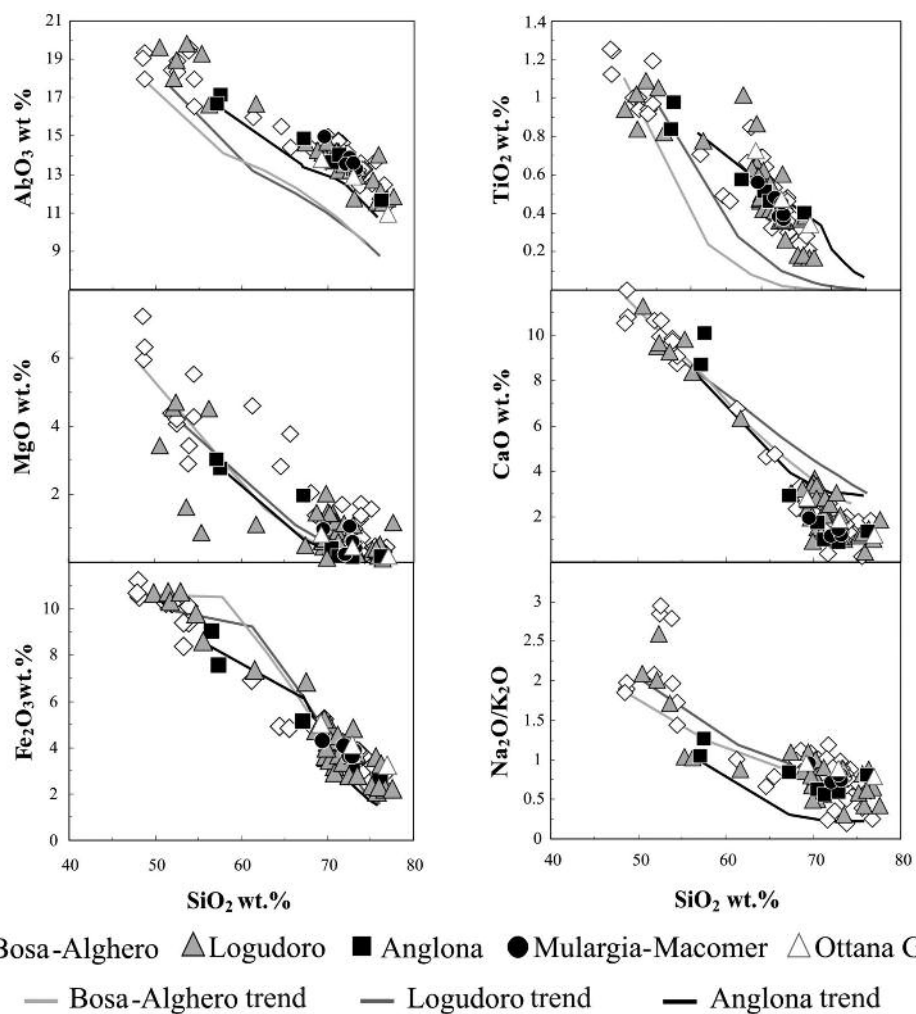


Figure 3. Selected major element variation diagrams for the studied Early Miocene volcanic rocks from northwestern Sardinia. The best-fit results of MELTS modelling for each volcanic district are also reported (see text for further explanations).

plagioclase, euhedral brown mica microcrysts, corroded clinopyroxene, quartz, rare subhedral green-brown amphibole and orthopyroxene, plus alkali feldspar and opaque oxides. Common accessories are zircon and apatite. Occasionally, secondary minerals such as zeolites, glauconite

and chlorite are observed.

b) Welded ignimbrites. These rocks show textures varying from eutaxitic to spherulitic, more rarely vitrophyric. The observed mineral phases are euhedral to subhedral plagioclase, subhedral clinopyroxene, rare rounded

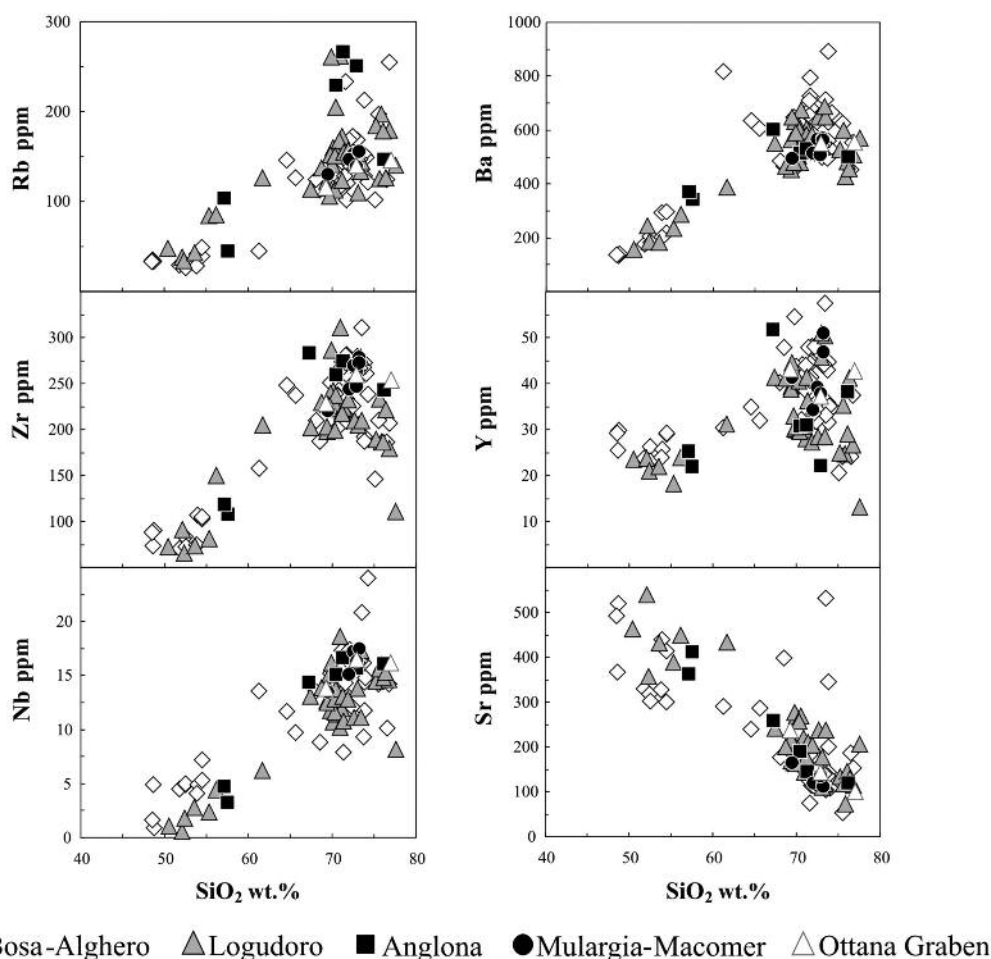


Figure 4. Selected trace element variation diagrams for the studied Early Miocene volcanic rocks from northwestern Sardinia.

orthopyroxene, apatite and opaque oxides included in mafic minerals or in isolated microcrysts. Subordinate microcrysts of alkali feldspar and quartz are also observed. The welded ignimbrites are characterized by the presence of volcanic fragments made principally of microcrystalline plagioclase, scoriae and deeply altered subhedral minerals (probably mafic phases).

Mineral and glass chemistry

Pyroxenes. The composition of the pyroxenes are reported in Table 3 and Figure 6. Bosa-Alghero and Anglona clinopyroxenes are essentially augitic ($\text{Ca}_{36-46}\text{Mg}_{40-42}\text{Fe}_{14-22}$ and $\text{Ca}_{38-43}\text{Mg}_{30-43}\text{Fe}_{19-27}$, respectively) with no substantial chemical differences between basaltic andesites and dacitic-rhyolitic welded ignimbrites. Logudoro basaltic

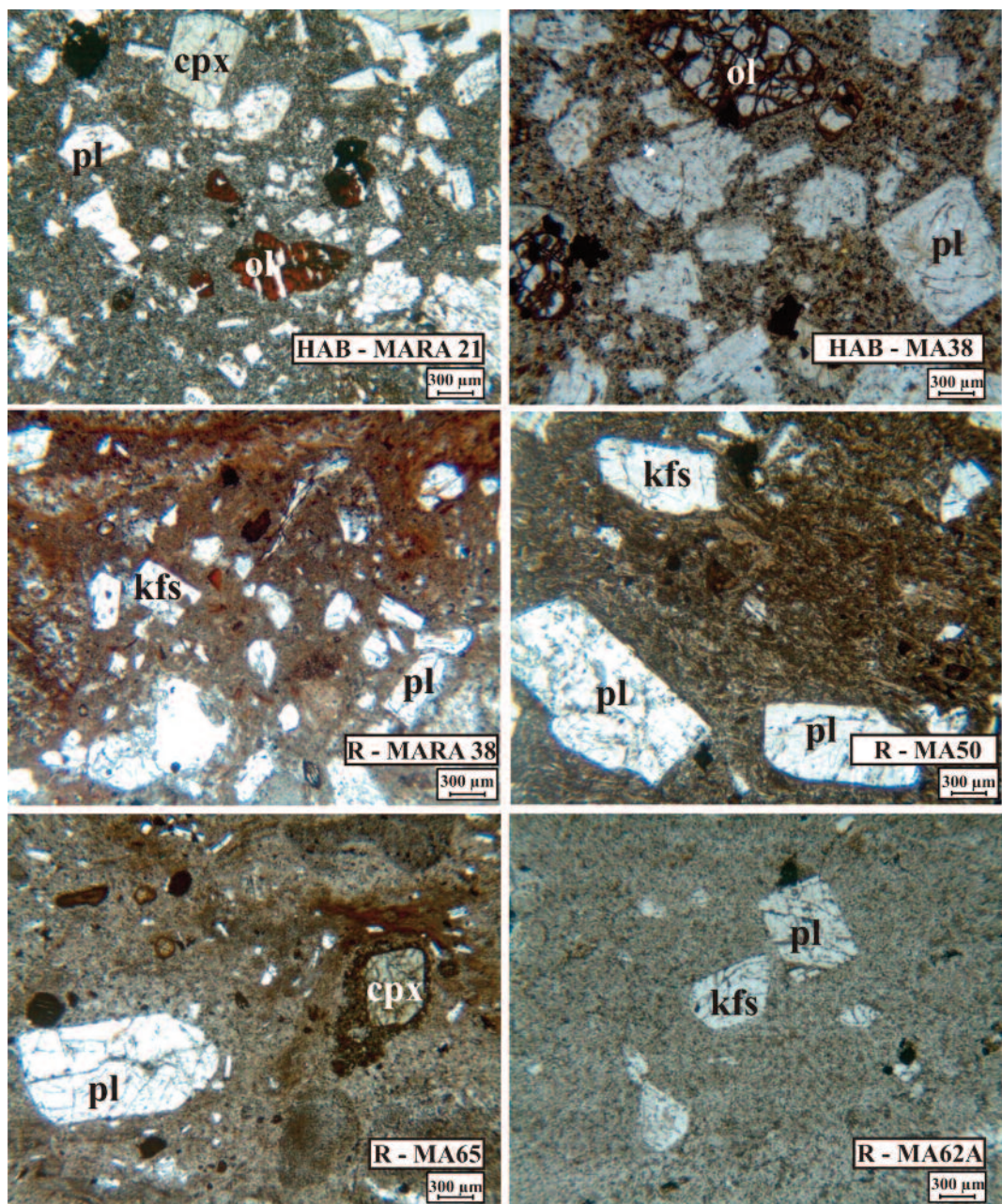


Figure 5. Thin section microphotographs for some representative samples of the studied Early Miocene volcanic rocks from northwestern Sardinia. ol = olivine; cpx = clinopyroxene; pl = plagioclase; kfs = alkali feldspar. HAB = high alumina basalt; R = rhyolite.

andesites have slightly Ca-richer and Fe-poorer clinopyroxenes ($\text{Ca}_{42-48}\text{Mg}_{37-41}\text{Fe}_{15-17}$). Mg# [$\text{Mg\#} = \text{Mg}/(\text{Mg}+\text{Fe})$] varies from 0.56 to 0.86. Orthopyroxene from the Bosa-Alghero dacites has variable Mg# (0.54 to 0.73; $\text{Ca}_3\text{Mg}_{53-70}\text{Fe}_{27-44}$), whereas orthopyroxene of the Anglona dacites have a narrower compositional spectrum and a generally Fe-richer composition (Mg# = 0.53-0.68; $\text{Ca}_{3.4}\text{Mg}_{50-64}\text{Fe}_{32-46}$). Orthopyroxenes of the Logudoro basaltic andesites and rhyolites have a rather homogeneous composition (Mg# = 0.59-0.65; $\text{Ca}_{2.3}\text{Mg}_{57-63}\text{Fe}_{34-41}$).

Feldspars. Plagioclase from the basalts and basaltic andesites of the Bosa-Alghero district show a wide compositional range from $\text{An}_{94}\text{Ab}_6\text{Or}_0$ to $\text{An}_{22}\text{Ab}_{74}\text{Or}_4$ (phenocrysts core and groundmass, respectively; Figure 7a; Table 4). Plagioclase of the Logudoro basaltic andesite shows a compositional range from $\text{An}_{88}\text{Ab}_{12}\text{Or}_0$ (phenocryst core) to $\text{An}_{52}\text{Ab}_{44}\text{Or}_3$ (groundmass). The andesites of the Anglona district are characterized by plagioclase with a moderate core-to-rim compositional variations ($\text{An}_{71-81}\text{Ab}_{19-29}\text{Or}_0$). Plagioclases from the more differentiated dacites and rhyolites show a wider compositional spectrum, ranging from labradorite to andesine and rare oligoclase ($\text{An}_{28-53}\text{Ab}_{45-67}\text{Or}_{2-5}$). Alkali feldspar occurs only in the most differentiated rocks (dacitic and rhyolitic) of the Bosa-Alghero, Anglona, Logudoro, Mulargia-Macomer and Ottana graben districts and range from K_2O -rich sanidine to anorthoclase ($\text{Ab}_{1-69}\text{An}_{1-16}\text{Or}_{15-97}$; Figure 7a).

Minor phases. *Opaque oxides* are present as magnetite and Ti-magnetite groundmass microcrystals showing variable ulvöspinel contents (mol. ulvöspinel = 0.13-0.41), and low ilmenite (mol. ilmenite = 0.81-0.91; Table 5).

Olivine crystals were analyzed in basalts and basaltic andesites from the Bosa-Alghero district and in basalts from the Logudoro district (Table 5). The analyses show a moderate compositional variation (e.g., Fo_{54-71}), high FeO (26.4-39.1 wt.%) and very low CaO (0.2-0.4 wt.%)

contents. More Mg-rich olivine compositions have been analyzed in the basalts of Montresta ($\text{Fo}_{87-89}\text{Fo}_{71}$; Morra et al., 1997).

Mica belongs to the phlogopite-annite series (Figure 7b; Table 6) and have a relatively low Mg# (0.34-0.52). Micas show relatively high Fe^{2+} (2.44-3.39 apfu) and low Ti contents (0.42-0.66 apfu) resulting in a reddish-brown colour of the crystals. Most micas are characterized by Fe^{3+} in the tetrahedral site, with values up to 0.27 apfu, but several have Al excess in the tetrahedral site so the remaining Al filled the octahedral site, with values up to 0.33 apfu (Figure 7b; Guarino et al., 2011).

Amphiboles, analyzed in rhyolitic rocks of the Logudoro district (Table 6), are thus classified as tschermakite plus rarer ferrohornblende and magnesiohornblende (Leake et al., 1997; Figure 7c) showing high Ca (1.69-1.83 apfu) contents. The Fe^{2+} ranges from 1.62 to 2.91 apfu and is associated with low Ti (0.17-0.31 apfu) and variable Mg# values [$\text{Mg}/(\text{Mg}+\text{Fe}^{2+})$] = 0.38-0.65].

Glass. The analyzed glasses of rhyolites from the Bosa-Alghero and Logudoro are rhyolitic. The Anglona glasses are basaltic andesites (in andesitic rocks) and rhyolites (in dacites; Figure 7d; Table 7).

Discussion and Conclusions

The Early Miocene volcanic rocks of northwestern Sardinia have a bimodal chemical composition, with dacitic/rhyolitic rocks being definitely predominant over basalts and andesites. The high alumina basalts (HABs) are a common lithotype of “orogenic” magmatism worldwide, whose genesis has been variously ascribed to high-degree partial melting of the subducted oceanic slab or low-pressure fractional crystallization of a high magnesium basalt (HMB) primitive magma (e.g., Kuno, 1960; 1968; Crawford et al., 1987; Myers, 1988; Sisson and Grove, 1993; Kersting and Arculus,

Table 3. Representative analyses and site occupancies (structural formulas calculated on 6 oxygens) for orthopyroxene (cpx) and clinopyroxene (cpx) crystals of Early Miocene rocks from northwestern Sardinia.

Rock type	Bosa-Alghero district						Anglona district						Logudoro district						
	BA	BA	BA	BA	R	R	A	D	D	D	A	D	BA	BA	R	BA	R	BA	R
MARA33	MARA33	MARA33	MARA33	MARA34	MARA29	MARA29	MA82	MA84B	MA84B	MA84B	MA82	MA84B	MA12	MA12	MA12	MA13A	MA13A	MA13A	MA13A
cpx	cpx	cpx	cpx	cpx	opx	opx	cpx	cpx	cpx	cpx	opx	opx	cpx	cpx	cpx	opx	opx	opx	opx
SiO ₂	51.19	49.43	49.11	49.25	52.45	54.11	51.23	51.42	51.23	51.58	51.27	53.13	51.55	52.42	47.01	53.90	53.40	51.54	51.81
TiO ₂	0.70	0.79	0.66	0.55	0.22	0.32	0.57				0.45	0.41		0.36		0.16	0.24	0.20	0.15
Al ₂ O ₃	1.61	4.52	3.82	1.41	0.60	1.23	2.32	1.19	1.08	1.22	2.16	1.22	1.40	7.61	1.26	0.69	0.72	0.63	
FeO	13.09	8.36	8.68	15.23	25.59	16.63	10.49	16.08	16.59	11.86	10.18	20.01	27.95	9.80	8.64	22.72	20.63	23.97	24.75
MnO	0.51	0.20	0.26	0.58	1.55	0.77	0.69	0.69	0.69	0.66	0.87	0.56	0.56	0.15	1.20	0.95	1.28	1.28	1.27
MgO	14.49	14.08	14.11	12.17	18.35	25.17	14.90	10.76	10.59	15.32	15.12	23.31	17.53	14.16	12.02	19.04	22.35	20.80	20.43
CaO	17.59	22.10	22.10	17.06	1.51	1.50	20.29	21.03	20.75	18.64	19.95	1.72	1.85	20.47	22.00	1.28	1.37	1.27	1.18
Na ₂ O	0.21	0.23	0.32	0.28	0.07	0.03						0.27	0.22	0.18	0.02	0.03	0.02		
Cr ₂ O ₃	0.03		0.06	0.04	0.05	0.05										0.02	0.02		
sum	99.4	99.7	99.1	96.5	100.4	99.8	99.8	101.2	100.9	99.1	100.1	100.4	99.4	97.7	99.7	99.7	99.8	100.2	
Si	1.934	1.837	1.836	1.940	1.995	1.975	1.913	1.951	1.952	1.945	1.925	1.960	1.973	1.968	1.769	2.000	1.991	1.943	1.952
^{IV} Al	0.066	0.163	0.164	0.060	0.005	0.025	0.087	0.049	0.048	0.054	0.075	0.040	0.027	0.032	0.231	0.009	0.032	0.028	0.021
Fe ³⁺																0.025	0.025		
Ti	0.020	0.022	0.019	0.016	0.006	0.009	0.016	0.015	0.004	0.000	0.013	0.012	0.010	0.038	0.005	0.007	0.006	0.004	
VI Al	0.006	0.035	0.005	0.006	0.022	0.028	0.015	0.015	0.004	0.000	0.020	0.013	0.001	0.029	0.107	0.056	0.021		
Fe ²⁺	0.378	0.159	0.128	0.460	0.814	0.508	0.288	0.465	0.481	0.345	0.288	0.589	0.869	0.305	0.209	0.719	0.643	0.731	0.759
Fe ³⁺	0.035	0.100	0.143	0.042			0.040	0.045	0.048	0.028	0.028	0.026	0.003	0.063					0.000
Mn	0.016	0.006	0.008	0.019	0.050	0.024		0.022	0.022	0.022	0.021	0.028	0.018	0.005	0.038	0.030	0.041	0.041	
Mg	0.816	0.780	0.786	0.715	1.041	1.370	0.829	0.609	0.601	0.861	0.846	1.282	1.000	0.792	0.674	1.075	1.242	1.169	1.147
Ca	0.712	0.880	0.886	0.720	0.061	0.059	0.812	0.855	0.847	0.753	0.802	0.068	0.076	0.823	0.887	0.052	0.055	0.051	0.047
Na	0.016	0.017	0.023	0.021	0.005	0.002	0.001	0.001						0.020	0.016	0.013	0.001	0.002	0.001
Cr	0.001													0.002	0.001				
Ca	36	46	45	37	3	3	41	43	42	38	41	3	4	42	48	3	3	3	2
Mg	42	40	36	53	70	42	30	43	43	64	50	41	37	57	63	58	57		
Fe	22	14	14	27	44	27	17	28	19	16	32	46	17	15	40	34	39	41	
Mg#	0.68	0.83	0.86	0.61	0.56	0.73	0.74	0.57	0.56	0.71	0.75	0.69	0.54	0.72	0.76	0.60	0.66	0.62	0.59

Mg# = Mg/Mg+Fe²⁺ gm = groundmass.

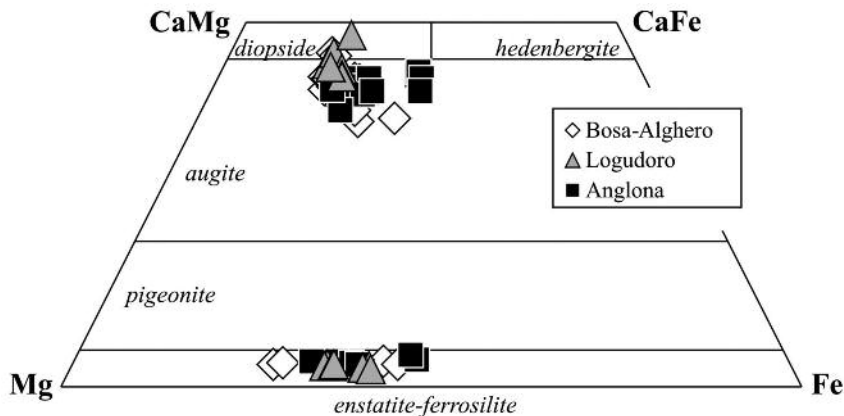


Figure 6. Classification of pyroxenes according to IMA rules (Morimoto et al., 1988).

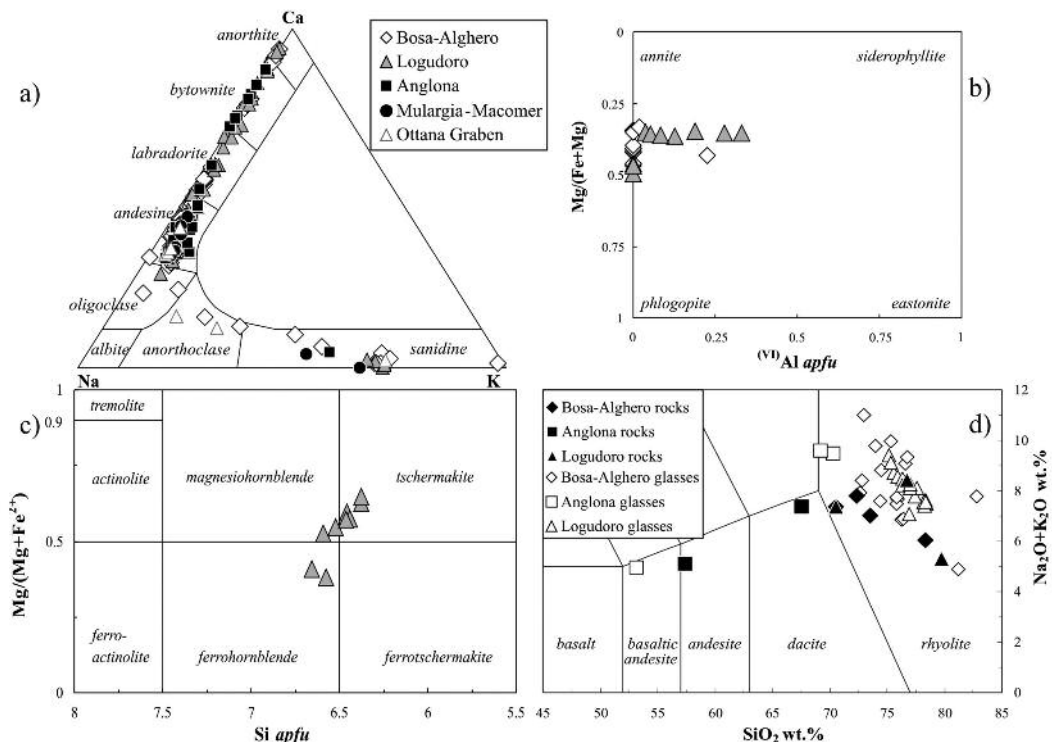


Figure 7. Classification diagrams for a) feldspar; b) brown mica (Deer et al., 1966); c) amphibole (Leake et al., 1997) and d) glasses (TAS, Le Bas et al., 1986) of the studied Early Miocene volcanic rocks from northwestern Sardinia.

Table 4. Representative analyses for feldspars of Early Miocene rocks from northwestern Sardinia.

Rock type	Bosa - Alghero district						Mularia-Macomer						Ottana graben district						
	HAB	HAB	BA	R	R	R	MARA23	MARA23	MARA33	MA29B	MA35	MARA15	MARA27	MARA38	MA62A	MA62A	MA62A	MA67	MA67
SiO ₂	57.72	63.71	44.01	56.37	57.91	67.77	57.37	70.09	57.78	58.18	66.84	57.78	66.84	60.04	59.65	60.04	59.65	66.91	66.91
Al ₂ O ₃	26.07	22.79	34.07	27.15	26.19	16.72	26.23	17.64	26.6	26.15	19.32	24.61	24.61	24.83	24.83	24.83	24.83	17.86	17.86
FeO	0.41	0.37	0.45	0.41	0.33	0.35	0.40	0.28	0.28	0.22	9.28	2.61	9.37	8.9	0.86	0.86	0.52	0.52	1.32
CaO	9.11	4.63	19.15	10.17	9.03	0.22	9.03	0.22	9.03	0.22	9.03	0.22	9.03	0.22	9.03	0.22	9.03	0.22	2.57
Na ₂ O	6.12	8.55	0.66	5.48	6.12	0.12	5.65	6.10	6.06	6.49	5.09	7.11	6.92	6.92	6.92	6.92	6.5	6.5	
K ₂ O	0.47	0.74	0.00	0.38	0.35	14.19	0.40	3.26	0.58	0.57	8.89	0.57	0.57	0.65	0.65	0.65	0.65	2.2	
sum	99.9	100.8	98.3	99.9	99.9	99.4	99.3	100.4	100.3	100.3	100.3	100.3	100.3	100.3	100.3	100.3	100.3	100.3	97.4
An%	44	22	94	50	44	1	46	15	45	42	4	45	42	4	33	33	35	35	15
Ab%	53	74	6	48	54	1	51	63	52	55	45	63	61	61	69	69	69	69	
Or%	3	4	0	2	2	97	2	22	3	3	51	4	4	4	4	4	4	4	16
Logudoro district																			
Rock type	Bosa - Alghero district						Mularia-Macomer						Ottana graben district						
	BA	BA	BA	R	R	R	MA12	MA12	MA12	MA13A	MA37	MA37	MA71	MA82	MA82	MA84B	MA84B	MA84B	
SiO ₂	46.22	46.02	49.96	54.79	55.53	62.40	65.36	44.8	47.53	49.67	59.4	59.4	57.02	57.02	57.02	57.02	57.02	57.02	59.15
Al ₂ O ₃	33.91	33.62	29.85	27.28	27.59	23.40	18.60	35.86	32.36	30.76	25.19	25.19	26.91	26.91	26.91	26.91	26.91	26.91	25.23
FeO	0.47	0.48	1.08	0.39	0.35	0.24	0.15	0.49	0.65	0.8	0.8	0.8	0.8	0.8	0.8	0.8	0.8	0.8	0.31
CaO	17.60	17.62	14.31	10.83	10.88	5.66	0.18	19.89	16.65	14.46	7.53	7.53	9.45	9.45	9.45	9.45	9.45	9.45	8.03
Na ₂ O	1.28	1.33	3.10	5.07	5.11	7.50	3.03	0.68	2.2	3.24	6.49	6.49	5.91	5.91	5.91	5.91	5.91	5.91	6.78
K ₂ O	0.05	0.07	0.22	0.57	0.40	0.93	11.78	100.1	101.7	99.4	99.9	99.9	100.1	100.1	100.1	100.1	100.1	100.1	100.1
sum	99.5	99.1	98.5	98.9	99.9	100.1	100.1	100.1	100.1	100.1	100.1	100.1	100.1	100.1	100.1	100.1	100.1	100.1	100.1
An%	88	88	71	52	53	28	1	94	81	71	36	36	45	45	45	45	45	45	38
Ab%	12	12	28	44	45	67	28	6	19	29	57	57	51	51	51	51	51	51	58
Or%	0	0	1	3	2	5	71	0	0	0	7	7	5	5	5	5	5	5	3

gm = groundmass An% = anorthite mol.% Ab% = albite mol.% Or% = orthoclase mol.%.

1994; Lopez-Escobar et al., 1997; Schiano et al., 2003). Dostal et al. (1982) were the first to deal with the genesis of northwestern Sardinia HABs, arguing for their non-primitive nature (mainly on the basis of their low Cr and Ni concentrations and Mg# values), but still considering them as a likely parental magma for the rocks of the calc-alkaline suite. Morra et al. (1997) pointed that the Montresta HMBs represent the most primitive magma of northwestern Sardinia (i.e., Mg# between 0.64 and 0.71, Cr ~ 294-737 ppm and Ni ~ 47-205 ppm), and the neighbouring HABs are related to HMBs through closed-system fractional crystallization processes. The chemical composition of the Sardinia HABs (e.g., $\text{Al}_2\text{O}_3 > 17.8 \text{ wt.\%}$, $\text{MgO} < 7.2 \text{ wt.\%}$, Mg# < 0.60, low Cr and Ni) can be similarly interpreted as unlikely primary melt compositions, but, rather, as melts derived from a more primitive HMB-like magmas. As a consequence, the HABs cannot be used to obtain information on mantle source characteristics. On the other hand, their possible parental linkage with the evolved rocks should be investigated in order to shed light on the low-pressure evolution processes in the area.

On the whole, major- and trace-element compositional trends, as well as mineral compositions, are quite coherent among the various districts, suggesting, at least qualitatively, a cogenetic relationship. Fractional crystallization of the mineral phases observed in thin section can, indeed, explain the gross features observed in Figures 3 and 4. The decrease of Al_2O_3 , MgO and CaO with increasing SiO_2 is compatible with removal of plagioclase and clinopyroxene plus olivine in the less evolved rocks. Orthopyroxene and alkali feldspar join the previous phases in the intermediate and evolved melts. This is particularly evident by the decrease of Rb and Ba at $\text{SiO}_2 \sim 70 \text{ wt.\%}$, a feature that suggests the onset of alkali feldspar fractionation roughly at the dacite-rhyolite transition. Similarly, the decrease of Zr and Y around $\text{SiO}_2 \sim 70 \text{ wt.\%}$

marks the onset of zircon fractionation. Scatter of data can be due to local differences between the various districts, the porphyritic character and/or to post-emplacement processes that may have modified mobile element contents. In addition, some role should have been also played by open-system differentiation processes, which are known to have acted in many other LEMM Sardinian districts (e.g., Narcao, Brotzu et al., 1997b; Sarroch, Conte, 1997; Sindia, Lonis et al., 1997; Montresta, Morra et al., 1997; Sant'Antioco, Conte et al., 2010; Figure 1b).

Quantitative models of fractional crystallization processes were tested by means of mass balance calculations, performed using the Stormer and Nicholls (1978) method. The results are summarized in Table 8. The transition from a HMB-type primitive magma (sample KB13; Morra et al., 1997) to the HABs of the Bosa-Alghero (MARA21) and Logudoro districts (MA72C) was tested, yielding satisfactory results ($\Sigma R^2 < 0.3$ for both; $\Sigma R^2 = \text{sum of square residuals}$) involving ~ 30-36% removal of a gabbroic assemblage made of 64% clinopyroxene ($\text{Ca}_{35}\text{Mg}_{46}\text{Fe}_{19}$), 22.8% plagioclase ($\text{An}_{91}\text{Ab}_9\text{O}_0$) and 13.2% olivine (Fo_{87}) for the Bosa-Alghero district, and of 60% clinopyroxene ($\text{Ca}_{45}\text{Mg}_{42}\text{Fe}_{13}$), 13.2% plagioclase ($\text{An}_{91}\text{Ab}_9\text{O}_0$) and 26.5% olivine (Fo_{71}) for the Logudoro district.

In the Bosa-Alghero district, the transition from HAB to basaltic andesite is modelled assuming ~ 43% of removal of a cumulate made of ~ 45% plagioclase ($\text{An}_{90}\text{Ab}_9\text{Or}_1$), ~ 32% clinopyroxene ($\text{Ca}_{41}\text{Mg}_{43}\text{Fe}_{16}$), ~ 13% olivine (Fo_{74}) and ~ 9% magnetite (Table 8). The transition from basaltic andesite to andesite is obtained after removal of 59.4% of a cumulate made of ~ 78% plagioclase ($\text{An}_{54}\text{Ab}_{43}\text{Or}_3$), ~ 12% clinopyroxene ($\text{Ca}_{39}\text{Mg}_{45}\text{Fe}_{16}$) and ~ 10% magnetite. The evolution from andesite to dacite was obtained after the removal of ~ 33% of a cumulate made of ~ 62% plagioclase ($\text{An}_{68}\text{Ab}_{30}\text{Or}_2$), ~ 29% orthopyroxene ($\text{Ca}_4\text{Mg}_{50}\text{Fe}_{46}$) and ~ 9% clinopyroxene ($\text{Ca}_{43}\text{Mg}_{42}\text{Fe}_{15}$).

Table 5. Representative analyses for olivine (ol), magnetite (mt) and ilmenite (ilm) crystals of Early Miocene rocks from northwestern Sardinia.

Rock type	Bosa - Alghero district						Anglona district				
	HAB	HAB	BA	BA	BA	BA	R	R	A	D	D
	MARA25 ol core	MARA25 ol rim	MARA 33 ol core	MARA 33 ol rim	MARA34 ol	MARA34 ol	MARA22 mt	MA29B ilm	MA82 mt	MA84B mt	MA3 ilm
SiO ₂	35.88	35.61	37.81	38.00	35.07	35.19		0.06			0.45
TiO ₂							17.81	46.46	11.59	7.01	41.01
Al ₂ O ₃							1.94	0.13	3.79	4.25	0.98
Fe ₂ O ₃							30.06	9.93	41.77	50.47	16.99
FeO	38.08	39.06	26.39	26.52	37.46	37.68	42.81	37.63	38.54	36.13	32.92
MnO	0.80	0.56	0.70	0.47	0.96	0.96	4.07	0.76		0.54	1.91
MgO	26.17	25.24	36.29	35.96	24.38	24.59		1.95	2.12	0.92	1.44
CaO	0.32	0.34	0.16	0.38	0.24	0.16					
sum	101.3	100.8	101.3	101.3	98.1	98.6	96.7	96.9	97.8	99.3	95.7
Fo	55	54	71	71	54	54					
ulvöspinel							0.35		0.22	0.13	
ilmenite								0.90			0.81

Fo% = forsterite mol%

Finally, the transition from dacite to a rhyolite was modelled with removal 55.5% of a solid assemblage made of plagioclase (~ 35%, An₄₅Ab₅₂Or₃), alkali feldspar (~ 31%, An₆Ab₄₀Or₅₄), clinopyroxene (~ 17%, Ca₃₉Mg₄₃Fe₁₈), orthopyroxene (~ 15%, Ca₃Mg₇₀Fe₂₇) and magnetite (~ 2%) (Table 8).

As for the Logudoro district, the transition from HAB to basaltic andesite is modelled with removal of 50.7% of a cumulate made of ~ 63% plagioclase (An₆₇Ab₃₁Or₂), ~ 21% clinopyroxene (Ca₄₀Mg₄₃Fe₁₇), ~ 7% magnetite and ~ 8% olivine (Fo₆₅). The transition from basaltic andesite to rhyolite was modelled with removal of ~ 74% of solid assemblage made of ~ 62% plagioclase (An₆₉Ab₃₀Or₁), ~ 15% clinopyroxene (Ca₃₀Mg₄₃Fe₂₇), ~ 10% alkali feldspar (An₄Ab₂₇Or₆₉), ~ 11% magnetite and ~ 1% apatite.

The transition from andesite to dacite in the Anglona district was obtained after removal

61.2% of a solid assemblage made of ~ 52% plagioclase (An₅₈Ab₃₉Or₃), ~ 29% clinopyroxene (Ca₄₀Mg₃₉Fe₂₁), ~ 11% alkali feldspar (An₄Ab₂₇Or₆₉) and 8% magnetite. The evolution from dacite to rhyolite is obtained removing 44.7% of a solid assemblage made of ~ 54% plagioclase (An₄₃Ab₅₄Or₃), ~ 24% alkali feldspar (An₂Ab₁Or₉₇), ~ 17% orthopyroxene (Ca₄Mg₆₄Fe₃₂) and ~ 6% magnetite.

Finally, the evolution from the dacitic to rhyolitic compositions in the Ottana graben district is modelled by 20.3% removal of plagioclase (52%, An₃₃Ab₆₃Or₄), alkali feldspar (22%, An₂Ab₂₇Or₇₁), clinopyroxene (13.3%, Ca₄₃Mg₃₀Fe₂₇), magnetite (9.8%) and orthopyroxene (2.9%, Ca₃Mg₅₅Fe₄₂). The evolution from two slightly different rhyolitic composition in the Mulargia-Macomer district is obtained through 24.8% of a solid assemblage made of 55.5% plagioclase (An₃₅Ab₆₀Or₅),

Table 5. Continued...

Rock type	Logudoro districts						Mulargia-Macomer district			Ottana graben district	
	HAB	BA	BA	R	R	R	R	R	R	R	R
	MA38 ol	MA72A mt	MA72A ilm	MA13A mt	MA13A ilm	MA13A ilm	MA50 mt	MA62A ilm	MA62A mt	MA67 mt	MA67 mt
SiO ₂	36.88	0.32		0.67	0.19	0.3		0.56			
TiO ₂		8.52	40.69	10.59	48.29	47.15	9.35	44.87	6.93	21.09	19.71
Al ₂ O ₃		1.49	1.76	1.94	0.17	0.17	1.43	0.87	1.35	1.2	1.44
Fe ₂ O ₃		46.99	16.49	44.73	8.20	10.60	47.18	6.90	53.93	24.89	24.61
FeO	29.28	36.62	30.77	40.49	38.71	36.79	37.53	39.95	37.68	48.89	46.65
MnO	0.46	0.01		0.77	1.13	3.29	0.7	1.07		1.08	0.89
MgO	31.91	0.93	3.27	0.49	2.14	1.49	0.46				
CaO	0.37										
<i>sum</i>	98.9	94.9	93.0	99.7	98.8	99.8	96.6	94.2	99.9	97.2	93.3
<i>Fo</i>	66										
<i>ulvöspinel</i>		0.17		0.20			0.18		0.13	0.41	0.40
<i>ilmenite</i>			0.81		0.91	0.89		0.90			

Fo% = forsterite mol%

30.1% alkali feldspar ($An_4Ab_{45}Or_{51}$), 8.5% orthopyroxene ($Ca_3Mg_{70}Fe_{27}$) and 5.9% magnetite.

Further informations on the evolutionary processes of Early Miocene rocks from northwestern Sardinia can be obtained from the estimation of T and fO_2 based on the mineral chemistry data (Table 9). The olivine-liquid geothermometer (Putirka, 2008) applied to olivine in the basalts and basaltic andesites from the Bosa-Alghero district gave temperatures in the range of 1071-1140 °C and of 1114 °C for the olivine in the basalts from the Logudoro district. The clinopyroxene-orthopyroxene geothermometer (Putirka, 2008) applied for pairs in equilibrium with the host rocks (i.e., $Fe/Mg K_d^{cpx-lid} = 0.27 \pm 0.03$; Putirka, 2008; Figure 8a), yielded temperatures between 931 and 964 °C for the Bosa-Alghero rhyolites, between 958 and 979 °C for the Anglona andesites and

between 934 and 1010 °C for the Anglona dacites.

Temperature and oxygen fugacity values for the Logudoro rhyolites were estimated on amphibole minerals following the method of Ridolfi et al. (2010). Temperature and oxygen fugacity ($\log fO_2$) range from 821 to 923 °C and from -10.7 to -13.6 log units, respectively. Similar T- fO_2 estimates were obtained by using coexisting magnetite-ilmenite pairs for samples from the Bosa-Alghero, Logudoro and Mulargia-Macomer districts. The Bosa-Alghero rhyolites gave temperature estimates spanning from 872 to 1035 °C and oxygen fugacity values ranging from -12.8 to -10.4 log units. As for the Logudoro rocks, basaltic andesites gave T values of 853-918 °C and oxygen fugacity of -12 to -11.1 log units, whereas rhyolites yielded temperature estimates spanning from 777 to 841.3 °C and oxygen fugacity from -14.8 to

Table 6. Representative analyses for mica and amphibole (amph) crystals of Early Miocene rocks from northwestern Sardinia. Also reported are site occupancies (structural formulas calculated on 22 oxygens for mica, 23 for amphiboles).

Rock type	Bosa-Alghero district						Logudoro district						
	R	R	R	R	MARA15 mica	MARA38 mica	MARA38 mica	MA37 mica	MA37 mica	MA13A mica	MA48B mica	MA71 mica	
SiO ₂	36.53	36.96	35.45	36.48	34.84	34.47	35.72	36.20	37.11	35.21	42.18	43.65	42.9
TiO ₂	4.95	3.91	4.269	5.27	4.15	3.76	4.52	5.70	3.55	3.53	2.73	2.44	1.45
Al ₂ O ₃	12.38	15.10	13.583	13.89	12.64	13.43	13.13	13.41	13.15	13.76	9.94	9.56	2.35
FeO	22.41	20.82	23.3	20.71	24.99	24.44	20.25	21.15	23.29	25.88	13.82	16.87	10.78
MnO	0.26	0.24	0.31	0.22	0.58	0.47	0.35	0.57	0.50	0.48	0.31	0.31	13.22
MgO	9.24	9.00	8.663	10.35	7.55	7.03	11.37	10.17	7.40	8.23	13	11.39	0.43
BaO	0.76	0.43	0.348	0.54	0.35	0.38	0.41	0.41	0.41	11.15	11.46	10.27	13.57
CaO	0.07	0.16	0.098	0.01	0.09	0.09	0.05	0.05	0.05	1.95	1.89	1.79	11.15
Na ₂ O	0.47	0.46	0.416	0.68	0.42	0.44	0.52	0.55	0.58	0.58	0.96	1.05	2.3
K ₂ O	8.17	7.76	7.966	8.60	8.41	7.88	8.73	8.78	8.07	8.71	0.22	0.22	0.73
F	0.55	1.01	2.12	0.75	0.37	0.47	0.53	0.53	0.53	0.53	0.3	0.3	0.52
<i>sum</i>		95.8	95.9	96.5	97.5	92.1	95.6	96.0	93.1	96.4	98.6	98.7	98.4
Mg#	0.43	0.44	0.42	0.48	0.35	0.34	0.52	0.46	0.36	0.63	0.55	0.38	0.65
Si	5.624	5.552	5.327	5.457	5.496	5.600	5.473	5.544	5.876	5.513	6.375	6.519	6.373
^{IV} Al	2.246	2.448	2.406	2.448	2.496	2.400	2.371	2.420	2.124	2.487	1.625	1.481	1.627
Fe ³⁺	0.130		0.268	0.094	0.008		0.156	0.036					
V ⁴⁺ Al		0.225							0.330	0.052	0.146	0.202	0.244
Ti	0.573	0.442	0.482	0.593	0.492	0.460	0.521	0.656	0.423	0.416	0.310	0.274	0.260
Fe ³⁺	2.755	2.616	2.658	2.496	3.288	3.320	2.438	2.673	3.084	3.389	1.747	2.107	1.625
Fe ²⁺	0.034	0.030	0.039	0.027	0.077	0.065	0.045	0.076	0.066	0.061	0.039	0.152	0.054
Mn	2.119	2.015	1.940	2.307	1.775	1.702	2.596	2.321	1.746	1.921	2.929	2.536	2.974
Mg													
Ba	0.045	0.025	0.020	0.031	0.022	0.024	0.025						
Ca	0.012	0.026	0.016	0.001	0.016	0.015	0.008						
Na	0.140	0.135	0.121	0.197	0.130	0.139	0.154	0.163	0.176	0.571	0.547	0.532	0.655
K	1.605	1.486	1.527	1.641	1.691	1.633	1.706	1.715	1.630	1.740	0.185	0.200	0.137
OH	3.732	3.519	2.993	3.648	3.816	3.761	3.743	4	4	1.895	2	1.855	1.758
F	0.268	0.481	1.007	0.352	0.184	0.239	0.257		0.105	0.145	0.145	0.242	

Mg# = Mg/(Mg+Fe²⁺).

Table 7. Representative glass analyses for Early Miocene rocks from northwestern Sardinia.

Bosa - Alghero district

<i>Rock type</i>	R	R	R	R	R	R	R	R	R	R	R	R	R
MA35	76.24	76.42	74.38	75.82	74.50	75.34	72.65	73.01	81.21	82.83	76.61	76.78	72.81
SiO ₂	0.15	0.15	0.04	0.13	0.35	0.09	0.41	0.09	0.13	0.00	0.19	0.16	0.31
TiO ₂	13.60	13.68	14.21	13.54	14.38	13.57	14.15	14.80	9.25	8.83	12.94	12.61	15.60
Al ₂ O ₃	1.65	1.44	2.11	1.58	0.83	0.27	2.41	0.49	3.08	0.16	0.43	0.39	0.82
FeO	0.07	0.06	0.00	0.08	0.00	0.07	0.10	0.00	0.02	0.00	0.00	0.00	0.00
MnO	0.17	0.14	0.24	0.18	0.01	0.00	0.44	0.03	0.05	0.00	0.00	0.01	0.03
MgO	1.29	1.21	1.42	1.15	1.10	0.64	1.93	0.56	1.35	0.42	0.72	0.62	2.03
CaO	2.45	2.41	2.60	2.37	3.25	3.37	3.63	3.34	2.93	1.95	3.02	2.79	4.27
Na ₂ O	4.39	4.49	4.98	5.10	5.58	6.59	4.28	7.65	1.97	5.82	6.06	6.53	4.14
K ₂ O	0.00	0.00	0.02	0.04	0.00	0.06	0.00	0.03	0.00	0.03	0.12	0.02	0.22
P ₂ O ₅	sum	100	100	100	100	100	100	100	100	100	100	100	100

Anglona district

<i>Rock type</i>	A	D	D	R	R	R	R	R	R	R	R	R	R
MA82	53.15	70.31	69.18	75.17	75.93	76.33	76.35	75.33	78.47	78.38	78.35	77.48	77.63
MA84B	0.00	0.47	0.54	0.12	0.14	0.00	0.14	0.20	0.00	0.00	0.00	0.04	0.00
MA84B	28.53	16.03	15.62	13.33	13.66	13.85	13.63	13.77	12.68	12.37	12.59	12.62	12.57
Al ₂ O ₃	1.10	2.30	3.04	1.10	0.74	0.60	0.79	0.71	0.54	0.65	0.42	1.06	0.85
FeO	0.00	0.19	0.05	0.07	0.07	0.00	0.07	0.06	0.00	0.00	0.00	0.16	0.00
MnO	0.00	0.10	0.46	0.12	0.00	0.00	0.00	0.00	0.00	0.00	0.01	0.06	0.02
MgO	12.25	1.11	1.45	0.71	0.78	0.75	0.79	0.75	0.83	0.96	0.89	0.70	0.66
CaO	4.56	4.43	3.91	2.99	2.86	2.76	2.49	2.84	2.44	2.58	2.43	2.71	2.99
Na ₂ O	0.42	5.06	5.68	6.41	5.68	5.71	5.73	6.28	5.04	5.06	5.15	5.05	5.11
K ₂ O	0.00	0.00	0.07	0.00	0.15	0.00	0.00	0.05	0.00	0.00	0.16	0.12	0.18
P ₂ O ₅	sum	100	100	100	100	100	100	100	100	100	100	100	100

Logudoro district

Table 8. Results of mass balance calculations for Early Miocene districts from northwestern Sardinia.

		<i>from</i>	<i>to</i>	ol	pl	cpx	opx	mt	kfs	ap	%f	ΣR^2
Bosa-Alghero district	KB13 (HMB, Morra et al., 1997)	MARA21 (HAB)	13.2	22.8	64.0						71.2	0.29
Logudoro district		MA72C (HAB)	26.5	13.2	60.3						64.0	0.30
Bosa-Alghero district	MARA21 (HAB)	MARA34 (BA)	13.2	45.4	32.4	9.0					56.7	0.49
	MARA34 (BA)	MARA36 (A)	77.9	12.3		9.8					40.6	0.32
	MARA36 (A)	MARA13 (D)	62.1	8.6	29.3						67.5	0.49
	MARA13 (D)	MARA38 (R)	34.7	17.0	14.8	1.9	31.5				44.5	0.18
Anglona district	MA82 (A)	MA84B (D)	51.9	28.8		8.0	11.3				38.8	0.35
	MA84B (D)	MA6A (R)	54.2		16.7	5.6	23.6				55.3	0.47
Logudoro district	MA72C (HAB)	MA72A (BA)	8.3	63.3	21.1		7.3				49.3	0.35
	MA72A (BA)	MA36 (R)	61.9	15.5		10.2	11.1	1.3			25.8	0.38
Mulargia-Macomer district	MA65 (R)	MA62A (R)		55.5		8.5	5.9	30.1			75.2	0.10
Ottana graben district	MA69 (D)	MA67 (R)		52.0	13.3	2.9	9.8	22.0			79.7	0.05

HMB = high magnesium basalt HAB = high alumina basalt BA = basaltic andesite A = andesite D = dacite R = rhyolite %f = wt.% of residual liquid R² = sum of squared residuals ol = wt.% of subtracted olivine pl = wt.% of subtracted plagioclase cpx = wt.% of subtracted clinopyroxene mt = wt.% of subtracted magnetic ilm = wt.% of subtracted ilmenite opx = wt.% of subtracted orthopyroxene kfs = wt.% of subtracted alkali feldspar ap = wt.% of subtracted apatite. See text for further explanations.

-12.9 log units. The rhyolites from the Mulargia-Macomer district gave temperature estimates in the range of 717-902 °C and oxygen fugacity values between -16.2 and -13 log units. Some magnetite-ilmenite pairs giving lower temperatures (< 800 °C), coupled with low oxygen fugacity values (up to -16.2 log units), probably represent re-equilibration effects, rather than original crystallization conditions. The same can be held as true for the temperature estimates obtained for the basaltic andesites from the Logudoro district, which seem to be too low for such relatively SiO₂-poor magmas.

The results of the temperature and oxygen fugacity calculations presented above show that most of the data for the Bosa-Alghero and Mulargia-Macomer districts plot close to or slightly above the Quartz-Fayalite-Magnetite (QFM) buffer, whereas the Logudoro rocks plot close to the Nickel-Nickel Oxide (Ni-NiO) buffer (Figure 8b).

The estimated temperatures are consistent with a genetic linkage among the various rocks. A negative correlation between temperature and SiO₂ can be observed, a feature compatible with the interpretation as a coherent liquid line of descent for each district. Some spread of values is present, and this can be due to different causes, including the use of T and fO₂ estimates based on different minerals or mineral pairs. However, we are confident that this does not significantly affect the reliability of the proposed model for magma evolution.

The oxygen fugacity and temperature data obtained on minerals were then used to fix the starting conditions for the application of the MELTS algorithm (Ghiorso and Sack, 1995) to the evolution of the studied Early Miocene rocks. The best-fit results of MELTS simulations are reported in Figure 3. The starting conditions are characterized by 1 kbar pressure, 0.2 wt.% of H₂O and QFM oxygen buffer for the Bosa-Alghero rocks, Ni-NiO oxygen buffer for the Logudoro and Anglona rocks. Such pressure

values, approximately correspond to a depth of 3 km, MELTS simulations performed using higher pressure values (2-5 kbar) resulted in the fractionation of a mineral assemblage which did not match the observed parageneses (e.g., no olivine). It is also to note that the the strongly evolved composition of the ignimbritic products may have been reached only after polybaric evolution.

The obtained best-fit trends (Figure 3) assume the following fractionating assemblages:

- Bosa-Alghero district: 79.3% removal of olivine (0.6% Fo₇₅Fa₂₅), clinopyroxene (22% Di₈₁Hd₁₉ to Di₅₀Hd₅₀), plagioclase (40.8% An₇₇Ab₂₃ to An₂₄Ab₇₆), alkali feldspar (1.5% Or), spinel (14.3%) and apatite (0.2%) for the transition from HAB to "rhyolitic" composition (~ 74 SiO₂ wt.%);

- Logudoro district: 73% removal of olivine (2.9% Fo₆₇Fa₃₃), clinopyroxene (11.9% Di₇₈Hd₂₂ to Di₅₀Hd₅₀), plagioclase (44.8% An₆₇Ab₃₃ to An₂₆Ab₇₄), alkali feldspar (0.9% Or), spinel (12.5%) and apatite (0.1%) for the transition from HAB to "rhyolitic" composition (~ 76 SiO₂ wt.%);

- Anglona district: 69.5% removal of clinopyroxene (13.5% Di₆₃Hd₃₇ to Di₅₁Hd₄₉), orthopyroxene (4.1% En₅₁Fs₄₉ to En₄₇Fs₅₃), plagioclase (40.1% An₅₄Ab₄₆ to An₄₀Ab₆₀), alkali feldspar (4.4% Or) and spinel (7.4%) for the transition from andesite to "rhyolitic" composition (~ 76 SiO₂ wt.%).

In summary, the fractionating assemblage obtained through MELTS (olivine ± clinopyroxene ± orthopyroxene ± plagioclase ± alkali feldspar ± spinel ± apatite) are generally consistent with petrography and mass balance calculations reported above, even though the difficulties in defining the exact starting conditions suggest that some parameters (e.g., P and H₂O contents) needs to be better constrained. The estimated evolutionary trends obtained by MELTS simulations are in quite good agreement with those shown by the studied Sardinian rocks

Table 9. Temperature (T, in °C) and oxygen fugacity ($\log f\text{O}_2$) estimates obtained from different methods for the studied Early Miocene volcanic rocks from northwestern Sardinia.

	<i>District</i>	<i>Rock type</i>	<i>Sample</i>	T (°C)	$\log f\text{O}_2$
magnetite-ilmenite pairs (IL-MAT Lepage, 2003)	Bosa-Alghero district	R	MA29B	872.3	-12.8
		R	MA29B	1035.1	-10.4
		BA	MA72A	918.4	-11.1
		BA	MA72A	853.0	-12.0
	Logudoro district	R	MA13A	828.7	-13.3
		R	MA13A	816.9	-13.5
		R	MA13A	786.8	-14.6
		R	MA13A	776.7	-14.8
		R	MA13A	841.3	-12.9
		R	MA13A	828.9	-13.1
	Mulargia-Macomer district	R	MA62A	866.2	-13.6
		R	MA62A	839.4	-14.0
		R	MA62A	901.9	-13.0
		R	MA62A	716.9	-16.2
Amphibole (Ridolfi et al., 2010)	Logudoro district	R	MA13A	856.3	-12.3
		R	MA13A	896.6	-11.4
		R	MA13A	919.0	-10.9
		R	MA13A	894.8	-11.6
		R	MA13B	883.2	-12.0
		R	MA37	832.5	-13.5
		R	MA37	922.7	-10.7
		R	MA37	821.2	-13.6
		R	MA37	890.0	-11.8
		HAB	MARA25	1109.8	
olivine-liquid geothermometer (Putirka, 2008)	Bosa-Alghero district	HAB	MARA25	1109.8	
		BA	MARA33	1139.9	
		BA	MARA33	1139.9	
		BA	MARA33	1139.9	
		BA	MARA34	1070.7	
		BA	MARA34	1070.7	
		HAB	MA38	1113.7	
		HAB	MA38	1113.7	
	Anglona district	R	MA29B	931.0	
		R	MA29B	953.1	
		R	MA29B	941.8	
		R	MA29B	964.3	
		A	MA82	979.5	
		A	MA82	957.9	
		D	MA84B	967.2	
		D	MA84B	967.7	
		D	MA84B	983.2	
		D	MA84B	951.0	
		D	MA84B	963.3	
		D	MA84B	1010.1	
		D	MA84B	934.3	

HAB = high alumina basalt BA = basaltic andesite D = dacite R = rhyolite.

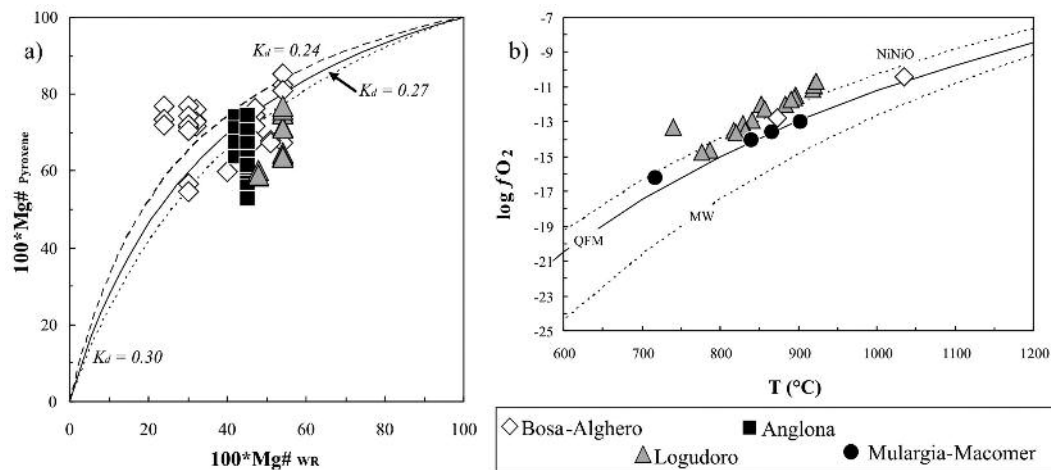


Figure 8. a) $100^*\text{Mg}^\#_{\text{Pyroxene}}$ vs. $100^*\text{Mg}^\#_{\text{WR}}$ diagram for Fe-Mg partitioning [$K_d = \frac{(\text{Fe/Mg})_{\text{px}}}{(\text{Fe/Mg})_{\text{WR}}}$] between pyroxene and whole rock of the studied Early Miocene rocks from northwestern Sardinia. b) $\log f\text{O}_2$ vs. T (in $^{\circ}\text{C}$) diagram for magnetite-ilmenite equilibrium pairs and amphiboles of the studied Early Miocene rocks from northwestern Sardinia.

for MgO , K_2O , Al_2O_3 (less evidently for the Bosa-Alghero district) and partly for the Fe_2O_{3t} (except for an anomalous peak at ~ 58 - 61 wt.% SiO_2 for the Bosa-Alghero and Logudoro districts; Figure 3). On the other hand, the very steep trend obtained for TiO_2 is likely due to the fact that MELTS assumes spinel crystallization in the initial evolutionary steps. The trends for CaO are remarkably good for the compositions up to 60 wt.% SiO_2 , whereas discrepancy exists for the most evolved rocks (which show CaO values close to zero, while MELTS simulations never reach concentrations below 2 wt.%).

In conclusion, the postulated genetic linkage between mafic and silicic rocks apparently rules out the early hypothesis of a crustal anatexis origin for the silicic Early Miocene rocks of Sardinia (e.g., Coulon et al., 1978; Beccaluva et al., 1987). Indeed, as previously observed by Morra et al. (1994) for the Sulcis area rocks, the widespread occurrence of the evolved rocks would have required unrealistically high degrees of partial melting. Such considerations, along

with the overall reliability of the above modelling, make the crustal anatexis model unlikely, even though a more detailed treatment of the matter (with isotopic data, geochemical modelling of partial melting of a crustal materials, and so on) will possibly give much stronger constraints. At the same time, the high amount of solid required to fractionate an original basaltic melt to reach rhyolitic compositions ($\sim 95\%$) remains hard to explain. Indeed, the huge amounts of dacitic and rhyolitic melts, if interpreted as the results of fractional crystallization would require huge amounts of cumulates (20,000 to 50,000 km^3) at shallow depths, not easy to be detected by geophysical studies. Also, open-system AFC-type processes must be appropriately taken into account, as their interplay seems likely given the local recognition of evidences of textural (e.g., crystals with corroded rims) and chemical (e.g., high Ca plagioclase in dacites and rhyolites) disequilibrium features.

The obtained results are preliminary basis for

further mineralogical, petrographic, chemical and isotopic investigations, which could help to shed new light on the petrogenesis of the silicic rocks in northwestern Sardinia, as well as on the whole LEMM magmatic cycle of Sardinia.

Acknowledgements

This paper is dedicated to the memory of prof. Enrico Franco, an incomparable professor of Mineralogy who forged generations of students and researchers with unfailing passion. A special thank goes to Prof. Pietro Brotzu, who taught and transmitted us his love and devotion to Sardinia. Thanks to the journal's scientific editor Antonio Gianfagna for the careful handling of the manuscript. The associated editors Maurizio de' Gennaro, Maria Rosaria Ghiara and Giuseppina Balassone (Napoli) are also thanked. The reviewers Michele Mattioli (Urbino University) and Aida Maria Conte (CNR, Rome) provided very constructive comments and suggestions. Marcello Serracino and Roberto de' Gennaro provided skilled help in the microprobe work. This work has been supported by research grants to Vincenzo Morra (MIUR-PRIN 2008, research grant#: 2008HMHYFP_003) and Michele Lustrino (University La Sapienza-AST 2008, 2009 and MIUR-PRIN 2008, research grant#: 2008HMHYFP_005).

References

- Araña V., Barberi F. and Santacroce R. (1974) - Some data on the comendite type area of S. Pietro and S. Antioco islands, Sardinia. *Bulletin of Volcanology*, 38, 725-736.
- Beccaluva L., Civetta L., Macciotta G. and Ricci C.A. (1985) - Geochronology in Sardinia: results and problems. *Rendiconti Società Italiana di Mineralogia e Petrologia*, 40, 57-72.
- Beccaluva L., Brotzu P., Macciotta G., Morbidelli L., Serri G. and Traversa G. (1987) - Cainozoic tectono-magmatic evolution and inferred mantle sources in the Sardo-Tyrrhenian area. In: *The lithosphere in Italy: Advances in Earth Science Research*. Accademia Nazionale dei Lincei, Roma, 229-248.
- Brandano M., Brilli M., Corda L. and Lustrino M. (2010) - Miocene C-isotope signature from the central Apennine successions (Italy): Monterey vs. regional controlling factors. *Terra Nova*, 22, 125-130.
- Brandano M. and Policicchio G. (2011) - Strontium stratigraphy of the Burdigalian transgression in the Western Mediterranean. *Lethaia*, in press, doi: 10.1111/j.1502-3931.2011.00285.x.
- Brotzu P., Lonis R., Melluso L., Morbidelli L., Traversa G. and Franciosi L. (1997a) - Petrology and evolution of calc-alkaline magmas from the Arcuentu volcanic complex (SW Sardinia, Italy). *Periodico di Mineralogia*, 66, 151-184.
- Brotzu P., Callegari E., Morra V. and Ruffini R. (1997b) - The orogenic basalt-andesite suites from the Tertiary volcanic complex of Narcao, SW-Sardinia (Italy): petrology, geochemistry and Sr-isotope characteristics. *Periodico di Mineralogia*, 66, 101-150.
- Carminati E., Wortel M.J.R., Spakman W. and Sabadini R. (1998) - The role of slab detachment processes in the opening of the Western-Central Mediterranean basins: some geological and geophysical evidence. *Earth and Planetary Science Letters*, 160, 651-665.
- Carminati E., Lustrino M., Cuffaro M. and Doglioni C. (2010) - Tectonics, magmatism and geodynamics of Italy: what we know and what we imagine. In: M. Beltrando, A. Peccerillo, M. Mattei, S. Conticelli and C. Doglioni (Eds.) *The geology of Italy: tectonics and life along plate margins*. *Journal of the Virtual Explorer*, 36, paper 9, doi: 10.3809/jvirtex.2010.00226.
- Cherchi A., Mancin N., Montadert L., Murru M., Putzu M.T., Schiavinotto F. and Verrubbi V. (2008) - The stratigraphic response to the Oligo-Miocene extension in the western Mediterranean from observations on the Sardinia graben system (Italy). *Bulletin de la Société Géologique de France*, 179, 267-287.
- Conte A.M. (1997) - Petrology and geochemistry of Tertiary calc-alkaline magmatic rocks from the Sarroch district (Sardinia, Italy). *Periodico di Mineralogia*, 66, 63-100.
- Conte A.M., Palladino D.M., Perinelli C. and Argenti E. (2010) - Petrogenesis of the High-Alumina Basalt-Andesite suite from Sant'Antioco Island, SW Sardinia, Italy. *Periodico di Mineralogia*, 79, 27-55.

- Coulon C., Baque L. and Dupuy C. (1973) - Les andésites cénozoïques et les laves associées en Sardaigne Nord-Occidentale (Provinces du Logudoro et du Bosano) - Caractères minéralogiques et chimiques. *Contributions to Mineralogy and Petrology*, 42, 123-139.
- Coulon C., Demant A. and Bellon H. (1974) - Premières datations par la méthode K-Ar de quelques laves cénozoïques et quaternaires de Sardaigne nord-occidentale. *Tectonophysics*, 22, 59-82.
- Coulon C. (1977) - Le volcanisme calco-alcalin cénozoïque de la Sardaigne (Italie): pétrographie, géochimie et genèse des lavas andésitiques et des ignimbrites. Signification géodynamiques. Thèse Univ. Marseilles, 1-370.
- Coulon C., Dostal J. and Dupuy C. (1978) - Petrology and geochemistry of the ignimbrites and associated lava domes from NW Sardinia. *Contributions to Mineralogy and Petrology*, 68, 89-98.
- Crawford A.J., Falloon T.J. and Eggins S. (1987) - The origin of island arc high-alumina basalts. *Contributions to Mineralogy and Petrology*, 97, 417-430.
- Deer W.A., Howie R.A. and Zussman J. (1966) - An Introduction to the Rock Forming Minerals. Longman, Harlow, Essex, 528 pp.
- Deino A.J., Gattacceca J., Rizzo R. and Montanini A. (2001) - $^{40}\text{Ar}/^{39}\text{Ar}$ dating and paleomagnetism of the Miocene volcanic successions of Monte Furru (western Sardinia): Implications for the rotation history of the Corsica-Sardinia microplate. *Geophysical Research Letters*, 28, 3373-3376.
- Deriu M. (1962) - Stratigrafia, cronologia e caratteri petrochimici delle vulcaniti Oligoceniche in Sardegna. *Memorie Società Geologica Italiana*, 3, 675-706.
- Dieni I., Massari F. and Médus J. (2008) - Age, depositional environment and stratigraphic value of the Cuccuru 'e Flores Conglomerate: insight into the Paleogene to Early Miocene geodynamic evolution of Sardinia. *Bulletin de la Société Géologique de France*, 179, 51-72.
- Dostal J., Coulon C. and Dupuy C. (1982) - Cenozoic andesitic rocks of Sardinia (Italy). In: Thorpe R.S. (ed.), *Andesites*. John Wiley & Sons, 353-370.
- Downes H., Thirlwall M.F. and Trayhorn S.C. (2001) - Miocene subduction-related magmatism in Sardinia: Sr-Nd and oxygen isotopic evidence for mantle source enrichment. *Journal of Volcanology and Geothermal Research*, 106, 1-21.
- Franciosi L., Lustrino M., Melluso L., Morra V. and D'Antonio M. (2003) - Geochemical characteristics and mantle sources of the Oligo-Miocene primitive basalts from Sardinia: the role of subduction components. *Ophioliti*, 28, 105-114.
- Gattacceca J., Deino A., Rizzo R., Jones D.S., Henry B., Beaudoin B. and Vedeboin F. (2007) - Miocene rotation of Sardinia: new paleomagnetic and geochronological constraints and geodynamic implications. *Earth and Planetary Science Letters*, 258, 359-377.
- Ghiorso M.S. and Sack R.O. (1995) - Chemical transfer in magmatic processes IV. A revised and internally consistent thermodynamic model for the interpolation and extrapolation of liquid-solid equilibria in magmatic systems at elevated temperatures and pressures. *Contributions to Mineralogy and Petrology*, 119, 197-212.
- Guarino V., Azzone R.G., Brotzu P., Gomes C.B., Melluso L., Morbidelli L., Ruberti E., Tassinari C.C.G. and Brilli M. (2011) - Magmatism and fenitization in the Cretaceous potassium-alkaline-carbonatitic complex of Ipanema São Paulo State, Brazil. *Mineralogy and Petrology*, doi:10.1007/s00710-011-0168-4.
- Gueguen E., Doglioni C. and Fernandez M. (1998) - On the post-25 Ma geodynamic evolution of the western Mediterranean. *Tectonophysics*, 298, 259-269.
- Jolivet L., Faccenna C., Goffé B., Mattei M., Rossetti F., Brunet C., Storti F., Funiciello R., Cadet J.P., D'Agostino N. and Parra T. (1998) - Mid crustal shear zones in post orogenic extension: example from the northern Tyrrhenian Sea. *Journal of Geophysical Research*, 103, 12123-12161.
- Kersting A.B. and Arculus R.J. (1994) - Klyuchevskoy Volcano, Kamchatka, Russia: The role of high-flux recharged, tapped and fractionated magma chamber(s) in the genesis of High-Al₂O₃ from High-MgO basalt. *Journal of Petrology*, 35, 1-41.
- Kuno H. (1960) - High-Alumina basalt. *Journal of Petrology*, 1, 121-145.
- Kuno H. (1968) - Differentiation of basalt magmas. In: Hess H.H., Plodervaart A.A., (eds.), *Basalts: the Poldervaart treatise on rocks of basaltic composition*, 2, New York, Interscience, 623-688.
- Le Bas M.J., Le Maitre R.W., Streckeisen A. and

- Zanettin P. (1986) - A chemical classification of volcanic rocks based on the Total Alkali-Silica diagram. *Journal of Petrology*, 27, 745-750.
- Leake B.E., Woolley A.R., Arps C.E.S., Gilbert M.C., Grice J.D., Hawthorne F.C., Kato A., Kisch A.J., Krivovichev V.G., Linthout K., Laird J., Mandarino J.A., Maresch W.V., Nickel E.H., Schumacher J.C., Smith D.C., Stephenson N.C.N., Whittaker E.J.W. and Youzhi G. (1997) - Nomenclature of amphiboles: report of the subcommittee on amphiboles of the International Mineralogical Association, commission on new minerals and minerals names. *Canadian Mineralogist*, 35, 219-246.
- Lecca L., Lonis R., Luxoro S., Melis F., Secchi F. and Brotzu P. (1997) - Oligo-Miocene volcanic sequences and rifting stages in Sardinia: a review. *Periodico di Mineralogia*, 66, 7-61.
- Lepage L.D. (2003) - ILMAT: An Excel worksheet for ilmenite-magnetite geothermometry and geobarometry. *Computer and Geosciences*, 29, 673-678.
- Lonis R., Morra V., Lustrino M., Melluso L. and Secchi F. (1997) - Plagioclase textures, mineralogy and petrology of Tertiary orogenic volcanic rocks from Sindia (central Sardinia). *Periodico di Mineralogia*, 66, 185-210.
- Lopez-Escobar L., Frey F.A. and Vergara M. (1977) - Andesites and high-alumina basalts from the central-south Chile high Andes: Geochemical evidence bearing on their petrogenesis. *Contributions to Mineralogy and Petrology*, 63, 199-228.
- Lustrino M., Morra V., Melluso L., Brotzu P., d'Amelio F., Fedele L., Franciosi L., Lonis R. and Petteruti Liebercknecht A.M. (2004) - The Cenozoic igneous activity of Sardinia. *Periodico di Mineralogia*, 73, 105-134.
- Lustrino M. and Wilson M. (2007) - The circum-Mediterranean anorogenic Cenozoic igneous province. *Earth-Science Reviews*, 81, 1-65.
- Lustrino M., Melluso L. and Morra V. (2007a) - The geochemical peculiarity of "Plio-Quaternary" volcanic rocks of Sardinia in the circum-Mediterranean area. In: Beccaluva L., Bianchini G., Wilson M. (eds.), Cenozoic Volcanism in the Mediterranean Area, *Geological Society of America Special Paper*, 418, 277-301.
- Lustrino M., Morra V., Fedele L. and Serracino M. (2007b) - The transition between "orogenic" and "anorogenic" magmatism in the western Mediterranean area. The Middle Miocene volcanic rocks of Isola del Toro (SW Sardinia, Italy). *Terra Nova*, 19, 148-159.
- Lustrino M., Morra V., Fedele L. and Franciosi L. (2009) - The beginning of the Apennine subduction system in central-western Mediterranean: constraints from Cenozoic "orogenic" magmatic activity of Sardinia (Italy). *Tectonics*, 28, TC5016, doi:10.1029/2008TC002419.
- Lustrino M., Duggen S. and Rosenberg C.L. (2011) - The central-western Mediterranean: anomalous igneous activity in an anomalous collisional tectonic setting. *Earth-Science Reviews*, 104, 1-40.
- Mattioli M., Guerrera F., Tramontana M., Raffaelli G. and D'Atri M. (2000) - High-Mg Tertiary basalts in southern Sardinia (Italy). *Earth and Planetary Science Letters*, 179, 1-7.
- Melluso L., Morra V., Brotzu P., Tommasini S., Renna M.R., Duncan R.A., Franciosi L. and D'Amelio F. (2005) - Geochronology and petrogenesis of the Cretaceous Antampombato-Ambatovy complex and associated dyke swarm, Madagascar. *Journal of Petrology*, 46, 1963-1996.
- Melluso L., Srivastava R.K., Guarino V., Zanetti A. and Sinha A.K. (2010) - Mineral compositions and magmatic evolution of the Sung Valley ultramafic-alkaline-carbonatitic complex (NE India). *Canadian Mineralogist*, 48, 205-229.
- Montigny R., Edel J.B. and Thuizat R. (1981) - Oligo-Miocene rotation of Sardinia: K-Ar ages and paleomagnetic data of Tertiary Volcanism. *Earth and Planetary Science Letters*, 54, 261-271.
- Morimoto N., Fabries J., Ferguson A.K., Ginzburg I.V., Ross M., Seifert F.A., Zussman J., Aoki K. and Gottardi D. (1988) - Nomenclature of pyroxenes. *American Mineralogist*, 62, 53-62.
- Morra V., Secchi F.A. and Assorgia A. (1994) - Petrogenetic significance of peralkaline rocks from Cenozoic calc-alkaline volcanism from SW Sardinia, Italy. *Chemical Geology*, 118, 109-142.
- Morra V., Secchi F.A.G., Melluso L. and Franciosi L. (1997) - High-Mg subduction-related Tertiary basalts in Sardinia, Italy. *Lithos*, 40, 69-91.
- Myers J.D. (1988) - Possible petrogenetic relations between low- and high-MgO Aleutian basalts. *Geological Society of America Bulletin*, 100, 1040-1053.

- Oudet J., Münch Ph., Verati C., Ferrandini M., Melinte-Dobrinescu M., Gattaceca J., Cornèe J.J., Oggiano G., Quillèvèrè F., Borgomaner J. and Ferrandini J. (2010) - Integrated chronostratigraphy of an intra-arc basin: $^{40}\text{Ar}/^{39}\text{Ar}$ datings, micropalaeontology and magnetostratigraphy of the early Miocene Castelsardo basin (northern Sardinia, Italy). *Palaeogeography, Palaeoclimatology, Palaeoecology*, 295, 293-306.
- Putirka K. (2008) - Thermometers and barometers for volcanic systems. In: Putirka K, Tepley F (eds.), Minerals, Inclusions and Volcanic Processes. Reviews in Mineralogy and Geochemistry, 69, American Mineralogical Society, Washington, DC, 61-120.
- Ridolfi F., Renzulli A. and Puerini M. (2010) - Stability and chemical equilibrium of amphibole in calc-alkaline magmas: an overview, new thermobarometric formulations and application to subduction-related volcanoes. *Contributions to Mineralogy and Petrology*, 160, 45-66.
- Sau A., Lecca L., Lonis R., Secchi F. and Fercia M.L. (2005) - La seconda fase del rift Sardo: vulcanismo ed evoluzione dei sub-bacini di Ardara-Chilivani e Bonorva (Sardegna Settentrionale). *Bollettino Società Geologica Italiana*, 124, 3-20.
- Schettino A. and Turco E. (2006) - Plate kinematics of the Western Mediterranean region during the Oligocene and Early Miocene. *Geophysical Journal International*, 166, 1398-1423.
- Schiano P., Clocchiatti R., Boivin P. and Medard E. (2003) - The nature of melt inclusions inside minerals in an ultramafic cumulate from Adak volcanic center, Aleutian arc: implications for the origin of high-Al basalts. *Chemical Geology*, 203, 169-179.
- Sisson T.W. and Grove T.L. (1993) - Temperatures and H_2O contents of low-MgO high-alumina basalts. *Contributions to Mineralogy and Petrology*, 113, 167-184.
- Speranza F., Villa I.M., Sagnotti L., Florindo F., Cosentino D., Cipollari P. and Mattei M. (2002) - Age of the Corsica-Sardinia rotation and Liguro-Provençal Basin spreading: new paleomagnetic and Ar/Ar evidence. *Tectonophysics*, 347, 231-251.
- Stormer J.C.J. and Nicholls J. (1978) - XLFrac: A program for the interactive testing of magmatic differentiation models. *Computer and Geosciences*, 4, 143-159.
- Vigliotti L. and Langenheim V.E. (1995) - When did Sardinia stop rotating? New paleomagnetic results. *Terra Nova*, 7, 424-435.

Submitted, August 2011 - Accepted, November 2011